



# Landslide susceptibility mapping by using a geographic information system (GIS) along the China–Pakistan Economic Corridor (Karakoram Highway), Pakistan

Sajid Ali<sup>1,2</sup>, Peter Biermanns<sup>1</sup>, Rashid Haider<sup>3</sup>, and Klaus Reicherter<sup>1</sup>

<sup>1</sup>Neotectonics and Natural Hazards, RWTH Aachen University, Lochnerstr. 4–20, 52056 Aachen, Germany

<sup>2</sup>Department of Earth Sciences, COMSATS Information Technology, Abbottabad, Pakistan

<sup>3</sup>Geological Survey of Pakistan, Islamabad, Pakistan

**Correspondence:** Sajid Ali (s.ali@nug.rwth-aachen.de)

Received: 12 February 2018 – Discussion started: 5 March 2018

Revised: 25 February 2019 – Accepted: 31 March 2019 – Published: 7 May 2019

**Abstract.** The Karakoram Highway (KKH) is an important route, which connects northern Pakistan with Western China. Presence of steep slopes, active faults and seismic zones, sheared rock mass, and torrential rainfall make the study area a unique geohazards laboratory. Since its construction, landslides constitute an appreciable threat, having blocked the KKH several times. Therefore, landslide susceptibility mapping was carried out in this study to support highway authorities in maintaining smooth and hazard-free travelling. Geological and geomorphological data were collected and processed using a geographic information system (GIS) environment. Different conditioning and triggering factors for landslide occurrences were considered for preparation of the susceptibility map. These factors include lithology, seismicity, rainfall intensity, faults, elevation, slope angle, aspect, curvature, land cover and hydrology. According to spatial and statistical analyses, active faults, seismicity and slope angle mainly control the spatial distribution of landslides. Each controlling parameter was assigned a numerical weight by utilizing the analytic hierarchy process (AHP) method. Additionally, the weighted overlay method (WOL) was employed to determine landslide susceptibility indices. As a result, the landslide susceptibility map was produced. In the map, the KKH was subdivided into four different susceptibility zones. Some sections of the highway fall into high to very high susceptibility zones. According to results, active faults, slope gradient, seismicity and lithology have a strong influence on landslide events. Credibility of the map was validated by landslide density analysis (LDA) and receiver oper-

ator characteristics (ROC), yielding a predictive accuracy of 72 %, which is rated as satisfactory by previous researchers.

## 1 Introduction

Landslides are a result of different geodynamic processes and represent a momentous type of geohazard, causing economic and social loss by damaging infrastructure and buildings (Vallejo and Ferrer, 2011). Landslides are mainly caused by conditioning and triggering factors. Conditioning factors include relief, lithology, geological structure, geomechanical properties and weathering, whereas precipitation, seismicity, change in temperature, and static or dynamic loads are triggering factors. Variations in these factors affect the occurrence of landslides. Heterogeneity in lithology influences hydrological and mechanical characteristics of rock mass. Slope morphology (curvature) depends upon lithology and structure within it. Size and type of mass movement changes with variations in lithology and structures. Some lithologies are more permeable and allow water to infiltrate and to increase the pore water pressure. This increase in pore water pressure during rainfall events ultimately affects shear strength of the rock mass and slope stability (Barchi et al., 1993; Cardinali et al., 1994), whereas the less pervious rock masses have low infiltration and high runoff leading to debris and mud flows (Dramis et al., 1988; Ellen et al., 1993; Canuti et al., 1993). Sheared and highly jointed rock masses contain shallow slope failures, whereas rockfalls are concen-

trated in well-bedded massive rock masses (Hu and Cruden, 1993). Distance from a tectonic feature has an inverse relation with rock fracturing and degree of weathering (Pradhan et al., 2010). State of weathering and fracturing makes slopes unstable (Ruff and Czurda, 2008). Slope is an important driving parameter for slope failures in the same geological and climatic setting (Coco and Buccolini, 2015). Shear strength decreases with increase in slope. Therefore, landslide density increases with increase in steepness (Pradhan et al., 2010). Kartiko et al. (2006) found that more than half of the landslides occur in areas where the slope is greater than 25 %. Curvature expresses the shape of the slope. If it is positive, then slope will be upwardly convex and will be concave in the case of a negative value. The later has the ability to retain water for longer time leading to increase in pore water pressure and hence in slope failures (Pradhan et al., 2010). Assessment of risks related to landslides was a long-term challenge for geologists but was significantly facilitated with the eventual availability of remote sensing (Shahabi and Hashim, 2015). Preparation of landslide inventory maps, acquisition of geomorphological data (elevation, slope, slope curvatures, aspect), hydrological parameters and extraction of lineaments from remote sensing products is now comparatively an easier task.

Landslide susceptibility mapping is the spatial prediction of landslide occurrence by considering causes of previous events (Guzzetti et al., 1999). It largely depends upon knowledge of slope movement and controlling factors (Yalcin, 2008). It has hitherto been carried out by many researchers in order to denominate potential landslide hazard zones through evaluation of responsible factors (Basharat et al., 2016; Komac, 2006; Lee et al., 2002, 2004; Shahabi and Hashim, 2015; Süzen and Doyuran, 2004). Preparation of their maps was based broadly on qualitative and quantitative approaches. Early research work (Nilsen et al., 1979) was largely quantitative, utilizing deterministic and statistical correlations and regression analysis of landslides and their controlling factors. In this context, safety factors, calculated on the basis of engineering parameters, are adduced to imply deterministic methods. In more recent works, statistical methods are favoured, attempting to draw correlations between spatial distribution of landslides and their controlling factors. Among these are the analytical hierarchy process, bivariate and multi-variate methods, logistic regression neural networks, fuzzy logic, etc. (Basharat et al., 2016; Guzzetti et al., 1999; Komac, 2006; Lee et al., 2002, 2004; Shahabi and Hashim, 2015; Süzen and Doyuran, 2004). These techniques were proven to be better options for comparatively large and complex areas (Cardinali et al., 2000). Expert opinion and landslide inventories are the decisive components of qualitative approaches (Yalcin, 2008). In most cases, landslide inventories were adduced to estimate failure susceptibility based on previous hazards in locations with similar geological, geomorphological and hydrological set-ups. Some geoscientists (Ahmed et al., 2014; Ayalew et al., 2004; Basharat

et al., 2016; Kamp et al., 2008; Kanwal et al., 2016; Shahabi and Hashim, 2015; Yalcin, 2008) incorporated statistical techniques (Analytical Hierarchy Approach, AHP, with weighted linear combination, WLC, and weighted overlay method, WOM) into qualitative methods to provide the identified factors with a numerical weighting. The combination of AHP and weighted overlay method (WOM) was termed as multiple-criteria decision analysis (MCDA) (Ahmed, 2015; Basharat et al., 2016; Kanwal et al., 2016). AHP is a simple and flexible method to analyse and solve complex problems (Saaty, 1987, 1990). It facilitates the estimation of influence that different factors might have on landslide development by comparing them in possible pairs in a matrix. This approach involves field experience and background knowledge of the researcher. A field campaign along the Karakoram Highway (KKH) in May 2016 enhanced our knowledge about factors controlling landslide events. Previous research considered MCDA as a better choice because of its accuracy to predict landslide hazard (Ahmed, 2015; Basharat et al., 2016; Kamp et al., 2008; Komac, 2006; Park et al., 2013; Pourghasemi et al., 2012). MCDA (combination of AHP with qualitative approaches) was declared a better option for regional studies (Soeters and van Westen, 1996). Previous wide usage in landslide susceptibility mapping, high accuracy, a simple process and flexibility according to local variation in landslide controlling parameters compelled us to choose this model. Furthermore, the use of a geographic information system (GIS) facilitated the extraction of geomorphic and hydrological parameters required for susceptibility assessment. Digital elevation models (DEMs) are commonly processed in GIS to extract crucial parameters for susceptibility assessment such as elevation, slope, aspect, curvature, watershed, etc. (Ayalew et al., 2004, 2005; Basharat et al., 2016; Ohlmacher and Davis, 2003; Rozos et al., 2011; Shahabi and Hashim, 2015; Süzen and Doyuran, 2004). Previously, landslide susceptibility maps of different fragments of northern Pakistan were prepared (Bacha et al., 2018; Basharat et al., 2016; Ahmed et al., 2014; Kamp et al., 2008; Kanwal et al., 2016; Khan et al., 2018; Rahim et al., 2018) (Table 1). They used a single model-based method, except two (Ahmed et al., 2014; Bacha et al., 2018) compared performances of two different models. Ahmed et al. (2014), Kanwal et al. (2016) and Rahim et al. (2018) used a regional geological map (1 : 500 000) to produce a landslide susceptibility map of the Upper Indus basin, whereas inventories were based on published rock avalanche maps (Kanwal et al., 2016), geomorphological mapping (Ahmed et al., 2014), co-seismic landslides (Basharat et al., 2016) and remote sensing along with field mapping (Bacha et al., 2018; Khan et al., 2018). Geological, geomorphological and human-induced parameters were also considered for production of susceptibility maps (Table 1).

**Table 1.** Previous work in some parts of northern Pakistan. MCE is multi-criteria evaluation, NDVI is normalized difference vegetation index, SPI is stream power index, TWI is topographic wetness index, WOE is weight of evidence, and FR is frequency ratio.

Authors	Method	Causative factors	Study area
Kamp et al. (2008)	MCE and AHP	aspect, elevation, faults, lithology, land cover, rivers, roads, slope, tributaries, aspect	Muzaffarabad District
Ahmed et al. (2014)	WOM and fuzzy logic	relief slope, curvature, aspect, rain, seismic hazard faults, drainage, NDVI, geology	Upper Indus watershed
Basharat et al. (2016)	MCE and AHP	aspect, elevation, faults, lithology, land cover, hydrology, roads, slope, curvature	BalaKot Tehsil
Kanwal et al. (2016)	AHP-based heuristic approach	slope, aspect, lithology, land cover, faults, road network, streams	Shigar and Shyok Basin in Karakoram range
Khan et al. (2018)	FR	slope, aspect, curvature, lithology, land cover, faults, road network, distance from stream, SPI, TWI	Haramosh valley, Bagrote valley and parts of Nagar valley
Bacha et al. (2018)	WOE, FR	aspect, fault, geology, land cover, proximity to road, slope, proximity to stream	Hunza–Nagar valley
Rahim et al. (2018)	AHP and WLC	slope, aspect, elevation, drainage network, SPI, TWI, lithology, fault lines, rainfall, road network, land cover, soil texture	Ghizer District
This study	AHP and WOM	elevation, slope angle, aspect, curvature, lithology, seismicity, faults, land cover, rainfall intensity and distance from streams	KKH (CPEC)

## 2 General situation of the study area

The Karakoram Highway (KKH), a part of the China–Pakistan Economic Corridor (CPEC), connects northern Pakistan with Western China (Fig. 1). It passes through rapidly rising mountain ranges of the Himalaya, Karakoram and Hindu Kush forming the junction between the Indian and Eurasian plates including the Kohistan Island Arc (Derbyshire et al., 2001). The area is characterized by fractured and weathered rock masses, diverse lithologies (igneous, metamorphic, and sedimentary), high seismicity, deep gorges, high relief, arid to monsoon climate and locally high rates of tectonic activity. These conditions make the study area a unique geohazards laboratory. Starting with its construction in 1979, KKH's stability has been endangered by a variety of geohazards.

The study area is the 840 km long (10 km buffer) Karakoram Highway (KKH), N35, located in the Karakoram Mountains, Himalaya. The area hosts some of the highest reliefs and highest peaks (Nanga Parbat: 8126 m, Rakaposhi: 7788 m) in the world (Hewitt, 1998). Goudie et al. (1984) termed the study area the steepest place on the earth where elevation drops from 7788 to 2000 m over a horizontal distance of 10 km (Fig. 2b, d).

From Abbottabad, the highway leads northwards through the sub-Himalayas entering the Indus Valley at Thakot, and the Hunza Valley at Gilgit, running parallel to the eponymous

rivers. From Thakot onwards, it passes through deeply incised valleys and gorges.

Weather conditions along the KKH are not uniform and are characterized by a wide range of annual mean temperatures ( $-5$  to  $46^{\circ}\text{C}$ ) and precipitation (15 to 1500 mm). The distribution of precipitation is additionally strongly fluctuating throughout the year. During the westerlies (January, February and March) and the monsoon period (July, August), the study area receives heavy rainfall. According to meteorological data, average annual precipitation between Abbottabad and Dasso is 1444 mm. However, north of Dasso, an abrupt change from monsoon to semi-arid to arid conditions is recorded which is owed to a change in valley orientation from north–south to east–west (Figs. 1 and 3). Furthermore, vertical climatic zonation exists in the Hunza Valley along the KKH. The surrounding peaks and slopes higher than 5000 m receive precipitation greater than 1000 mm per year, whereas the valley floor below is characterized by a semi-arid to arid climate (Hewitt, 1998).

The Karakoram and Himalaya host some of the world's longest continental glaciers with the steepest gradient and highest glacial erosion rates (Goudie et al., 1984). The snouts of some glaciers (Batura, Ghulkin, Pasu, Gulmit, Gulkin) are close to the KKH and partly cross it (Fig. 2a, c). Relatively warm temperatures in the valleys result in sudden melting of ice, frequent surges, catastrophic debris flows and blockage of rivers.

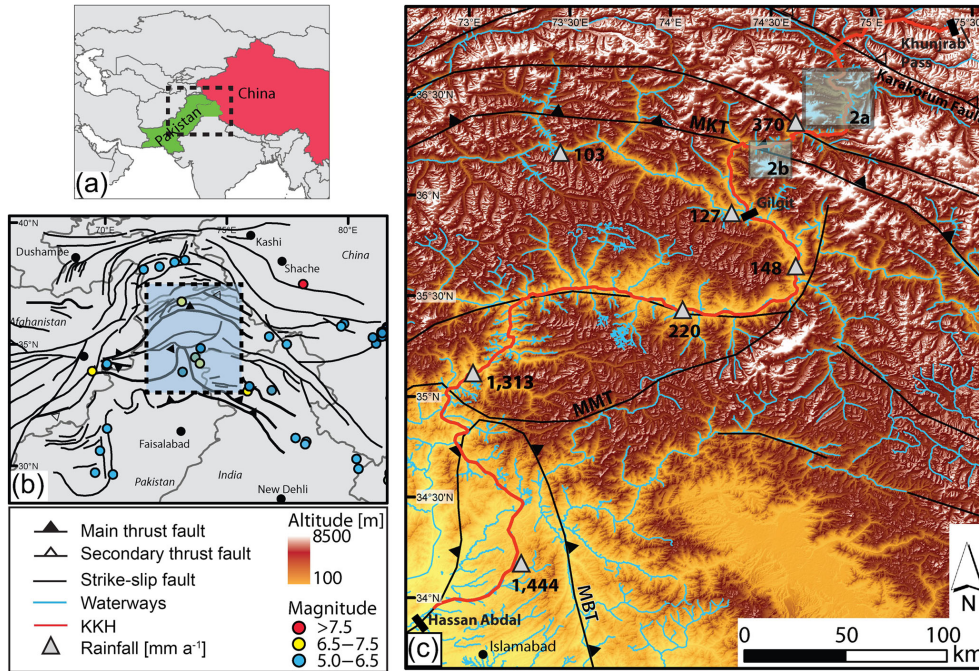


**Figure 1.** Overview of tectonics and precipitation in the study area. (a) Location of the study area in the region. (b) Active faults and major earthquake events in the region (USGS Earthquake Catalog, 2017). (c) Locations of the weather stations with mean annual rainfall (Pakistan Meteorological Department) and overview of tectonics and topography of the study area (After Hodges 2000): boxes 2a and 2b represent locations of Fig. 2. KKH is the Karakoram Highway, MBT is main boundary thrust, MMT is main mantle thrust, MKT is main Karakoram thrust (modified after Ali et al., 2017).

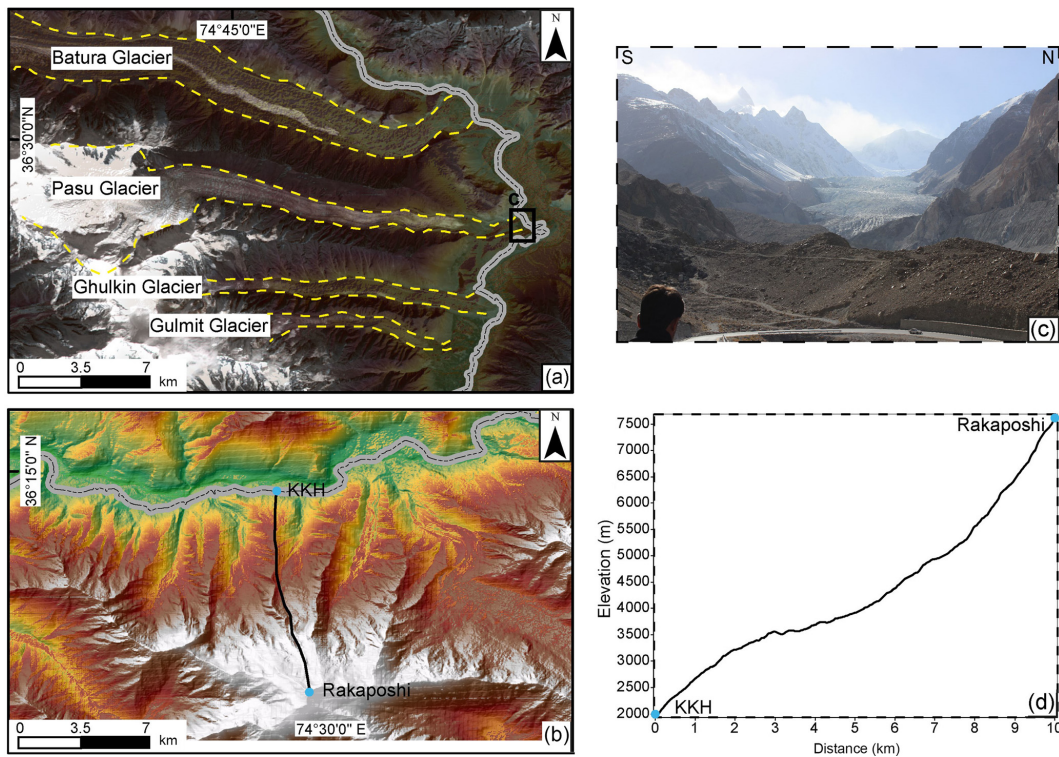


**Figure 2.** (a) Glaciers along the KKH. (b) Relief along the KKH. (c) Pasu Glacier's snout approaching the KKH. (d) Profile drawn along axis drawn in Fig. 2b: elevation drops from 7788 to 2000 m over a horizontal distance of 10 km.

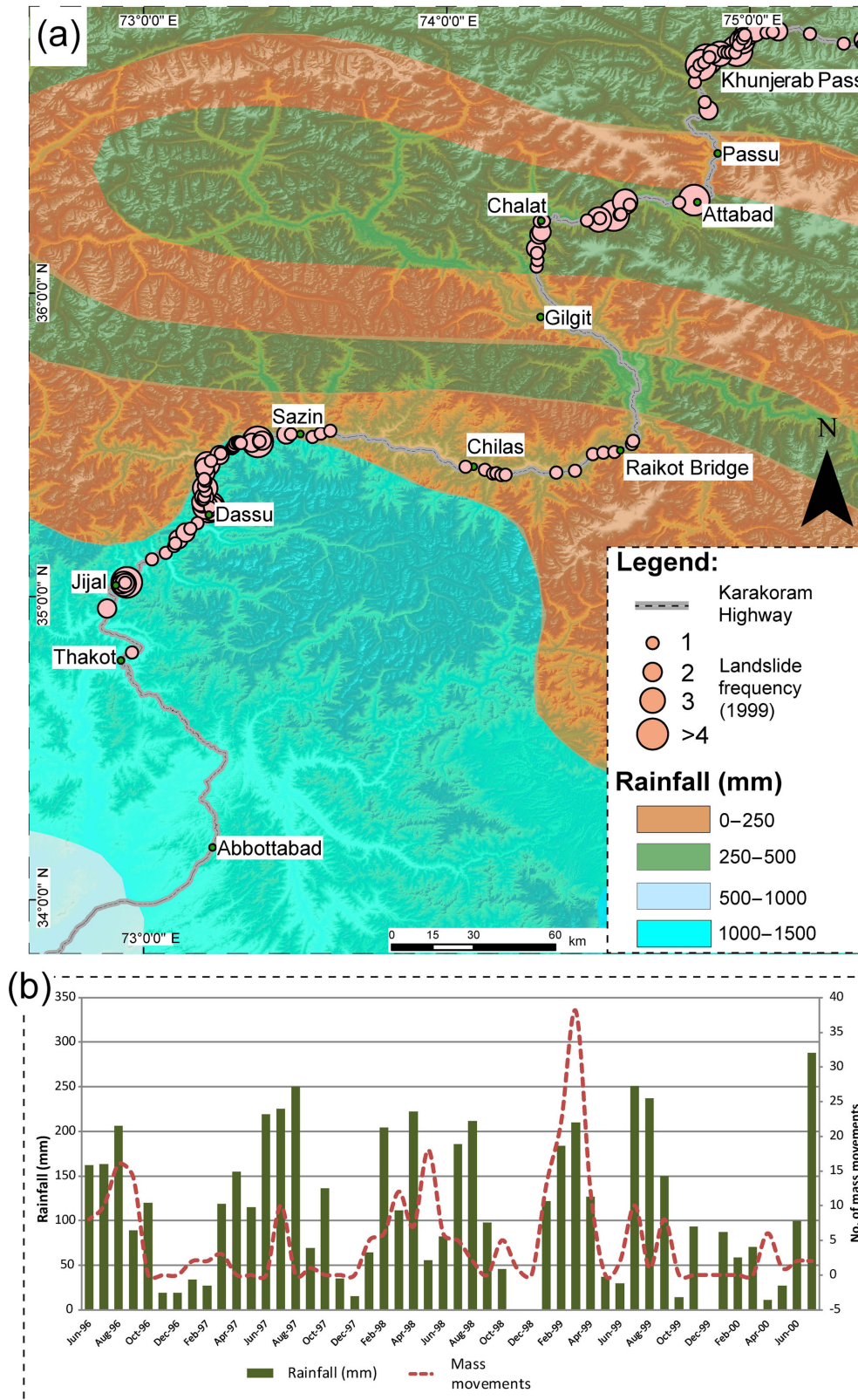


**Figure 3.** (a) Overview of precipitation (mean annual rainfall) and landslide frequency along the KKH (after Khan et al., 2000; Pakistan Meteorological Department 1982, 1983, 1996, 1997, 1998, 1999, 2000, 2014, 2015, 2016, Frontier Works Organization archives). (b) Correlation between landslide events and precipitation (Ali et al., 2017).

### 3 Geology along the KKH

Tectonically, the area is characterized by orogenic features that started forming with the onset of the Indo–Eurasian collision 50 Myr ago. Crustal shortening, subduction and active faulting are still ongoing with convergence rates of  $\sim 4$ – $5$  cm per year (Jade, 2004) and uplift rates of  $\sim 7$  mm per year (Zeitler, 1985). Main mantle thrust (MMT), Kamila Jal shear zone (KJSZ), Raikot Fault, main Karakoram thrust (MKT) and Karakoram Fault are important tectonic features responsible for brittle deformation along the highway (Fig. 4) (Bishop et al., 2002; Burg et al., 2006; DiPietro and Pogue, 2004; Goudie et al., 1984). Due to this brittle deformation, the rock mass is highly jointed and fractured. The general geology along the KKH consists of sedimentary, igneous and metamorphic rocks. Highly active landslide zones were identified from the multi-temporal landslide inventory of the KKH (Fig. 6). Jijal–Dassu, Raikot Bridge, Hunza Valley and Khunjerab valley sections are characterized by a large number of mass movements, and therefore a detailed geology is only discussed for these sections.

The geology of the Jijal–Dassu section is composed of ultramafic and low- to high-grade metamorphic rocks. The Mansehra granite, the Besham group, the Jijal Complex, the Kamila amphibolite and the Chilas Complex are important lithological units in this section. The Besham group comprises biotitic gneisses, cataclastic gneisses and quartzite, which were metamorphosed during the Himalayan orogeny  $\sim 65$  Myr ago (Ding et al., 2016). It shares a faulted contact with the Jijal Complex (Kohistan Island arc) along the northward dipping MMT (Williams, 1989). The ultramafic rocks with garnet granulites and Alpine-type metamorphic rocks between Jijal and Pattan are collectively termed as Jijal Complex (Tahirkheli and Jan, 1979). The Besham group shows signs of crushing of individual minerals and staining of quartz, whereas the Jijal Complex is massive and sheared (Khan et al., 1989). Owing to the contact of the Jijal Complex with the MMT in the north and the Pattan Fault in the south, it is highly tectonic and deformed. The Kamila amphibolite consists of sheared basic lavas and intrusive plutons (Treloar et al., 1996). It is classified into two types: garnet-bearing and garnet-free amphibolites. The former is massive and sheared due to the presence of Pattan and Kamila Jal shear zones (KJS), whereas the latter is banded. The garnet-free amphibolite shares a sheared contact with the Chilas Complex, mafic intrusions of predominantly gabbro-norites, sheared gabbro-norites and diorites (Searle et al., 1999).

The Raikot Bridge section exhibits continuous mass movement process because of its location at the seismically active western limb of the MMT known as Raikot Fault, a strike-slip fault with right-lateral movement. It is marked by a concentration of hot springs and a large shear zone. Granitic gneisses, quartzites, gabbro-norite, schists and Quaternary sediments are the main lithological units in this section. Contin-

uous erosion by the Indus River and highly deformed rocks are responsible for landslide events.

MKT is a part of the Hunza valley section and is responsible for many landslide events. The pre-dominant local lithologies of the Baltit Group, Chalt schists, Karakoram batholith as well as Quaternary sediments are highly tectonic and deformed.

The highly deformed Misgar slates, along with the Gujhal dolomite and Kilk formation, are the main components of the Sost section. The Karakoram fault is an important tectonic feature in this section. Highly fissile and closely jointed slates are important sources of scree on steep slopes along the highway. Intense weather conditions aggravate the situation in this section.

### 4 Seismology

The highway passes through one of the seismically most active areas in the world. The presence of active thrusts and strike-slip faults gives rise to earthquakes, anon triggering numerous landslides. The seismic activity along KKH is demonstrated by  $317M > 5$  and  $10M > 7$  recorded earthquake events (Muzaffarabad October, 2005:  $M = 7.6$ , Afghanistan October, 2015:  $M = 7.5$ ) since 1904 (Zhiquan and Yingyan, 2016). The highway passes through important seismic zones: the Indus Kohistan seismic zone (IKSZ), the Hamran seismic zone (HSZ), the Raikot–Sassi seismic zone (RSSZ) and the Yasin seismic zone (YSZ) (Fig. 4). The Jijal–Dassu section of the KKH passes through the northern part of IKSZ. IKSZ is 50 km wide and represents a highly active wedge-shaped structure containing a shallow and midcrustal zone (MonaLisa et al., 2009). The Muzaffarabad (2005,  $M = 7.6$ ) and Pattan earthquakes (1974,  $M = 6.2$ ) are recent destructive earthquakes in this seismic zone.

Sazin section of the highway is a part of HSZ, an active seismic zone hosting recent events with magnitudes of 3 to 6.2. The active Raikot Fault traverses RSSZ and is responsible for shallow seismicity of magnitudes 3 to 6.3. Both the fault and the KKH run, in direct vicinity, on the western banks of the Indus River. The YSZ encompasses the region surrounding the small town of Yasin. It is characterized by earthquakes with magnitudes between 3 and 5 and focal depths of less than 50 km. The MKT is suspected to be the main source of seismicity for this seismically active region.

### 5 Methodology

The flow chart (Fig. 5) describes the steps and techniques involved in preparation of the susceptibility map, involving multiple techniques, literature review, field observation and remote sensing.

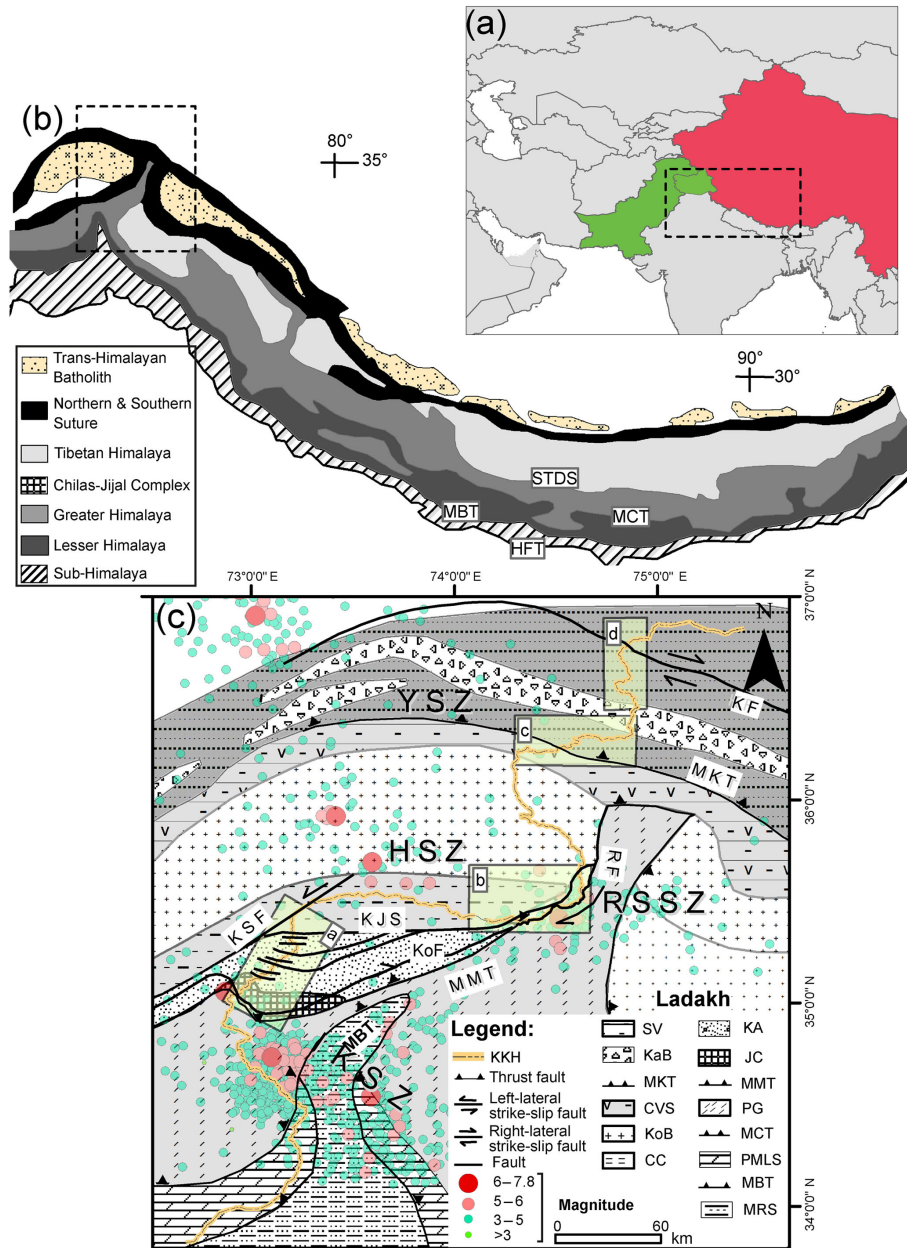


**Figure 4.** (a) Regional location of Himalaya. (b) Overview of Himalayan geology. (c) Geology along the KKH (compiled from Khan and Jan, 1991; Derbyshire et al., 2001; DiPietro and Pogue, 2004; DiPietro et al., 2000; Hewitt et al., 2011). Four boxes represent four sections (a is Jijal–Dassu section, b is Raikot Bridge section, c is Hunza Valley section and d is Khunjerab valley section). MMT is main mantle thrust, KJS is Kamila Jal shear zone, MKT is main Karakoram thrust, KF is Karakoram Fault, KSF is Kamila strike–slip fault, IKSZ is Indus Kohistan seismic zone, HSZ is Harman seismic zone, RSSZ is Raikot Sassi seismic zone, YSZ is Yasin seismic zone, SV is sediments and volcanics, KaB is Karakoram batholith, CVS is Chalt volcanics and schist, KoB is Kohistan batholith, CC is Chilas Complex, KA is Kamila amphibolites, JC is Jijal Complex, PG is Precambrian gneisses, PMLS is Palaeozoic and Mesozoic limestones and sandstones, MRS is Miocene redstones.

**5.1 Literature review**

In the first step, existing information and data for the study area were collected from archives of the Frontier Works Organization (FWO), Geological Survey of Pakistan (GSP), Pakistan Meteorological department (PMD) and research

catalogues (Khan et al., 2000). FWO is responsible for clearance and maintenance of the KKH after its potential blockage. Road maintenance logs were collected and digitized. The following three important maps were prepared from data collected:

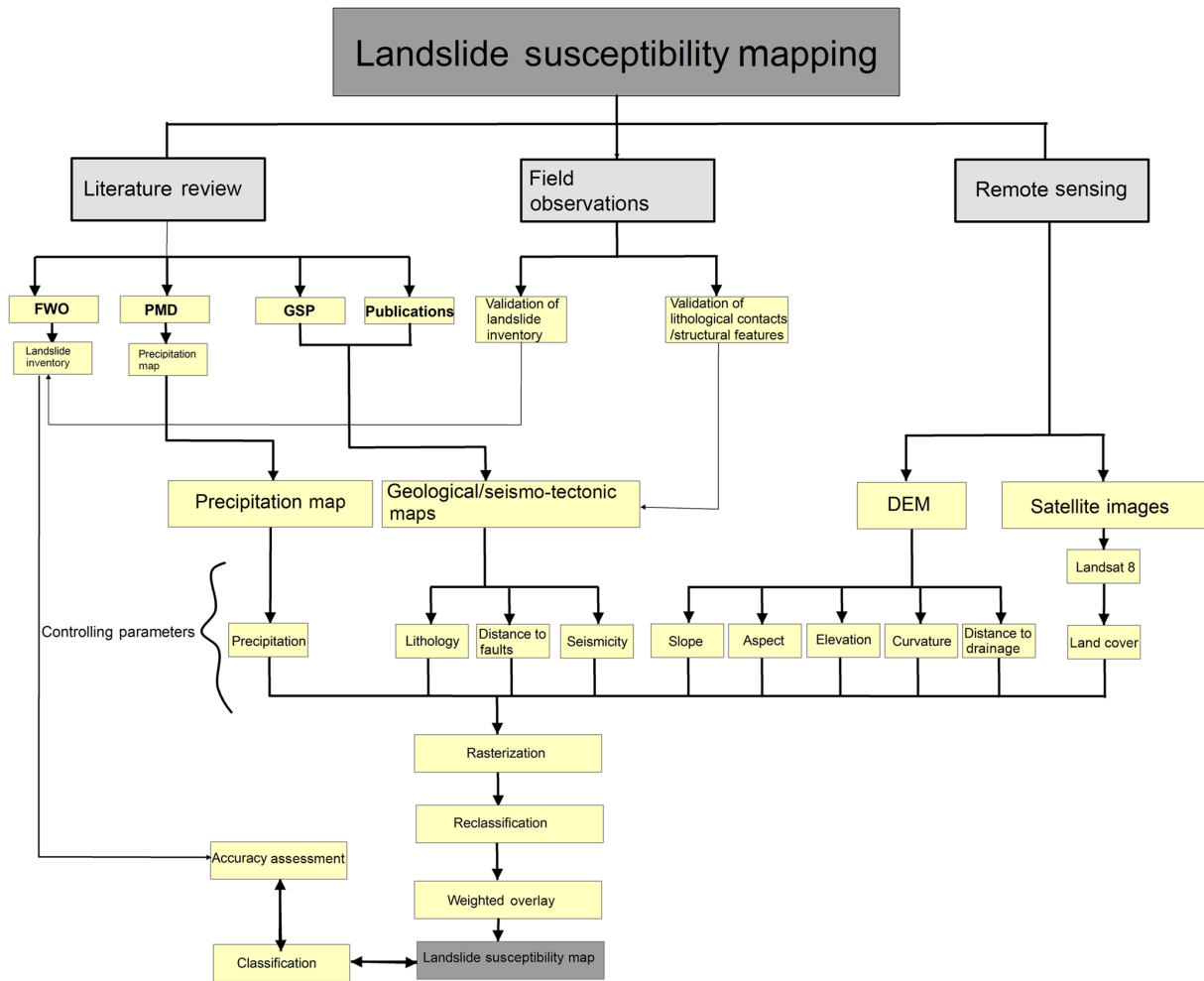


**Figure 5.** Flow chart showing multiple steps involved in the preparation of the susceptibility map: FWO is Frontier Works Organization, PMD is Pakistan Meteorological Department, GSP is Geological Survey of Pakistan and DEM is digital elevation model.

- i. A multi-temporal landslide inventory map (Fig. 6) was prepared using GIS, based on GSP's publications (Fayaz et al., 1985; Khan et al., 1986, 2003) and road maintenance logs of FWO.
- ii. A comprising geological and seismo-tectonic map (1:50 000 and 1:250 000) of the area was prepared by digitizing and compiling various pre-existing maps (Khan et al., 2000). Data related to lithology, faults and seismicity have been extracted from these maps.
- iii. An annual precipitation map of the study area was prepared by using rainfall data of six weather stations and previous map (Figs. 1 and 3) along the KKH.

### Landslide inventory

A landslide inventory map is an important instrument to display the location, date of occurrence and type of mass movement (Guzzetti et al., 2012). Landslide inventory maps are

prepared to define and record the extent of mass movements in different regions; to investigate an impact of lithology, geological structures (fault, fold, etc.) on types, distribution and occurrence of landslides; to use for preparation of landslide susceptibility mapping; and to analyse geomorphic evolution of an area. Preparation of these maps involves multiple techniques based on satellite imagery, field interpretations and compilation of previous publications (Guzzetti et al., 2000; van Westen et al., 2006).

In this study, we used real-time data of landslide occurrences acquired from road clearance logs of Frontier Works Organization (FWO) for different periods (1982, 1983, 1996, 1997, 1998, 1999, 2000, 2014, 2015, 2016), publications of Geological Survey of Pakistan (GSP) (Fayaz et al., 1985; Khan et al., 1986, 2003), a research article (Hewitt, 1998), Google Earth imagery and field surveys to prepare a multi-temporal landslide inventory along the highway (Fig. 6). Polygon outlines for clearly visible landslides on satellite imagery (based on data of FWO and GSP) were drawn. This



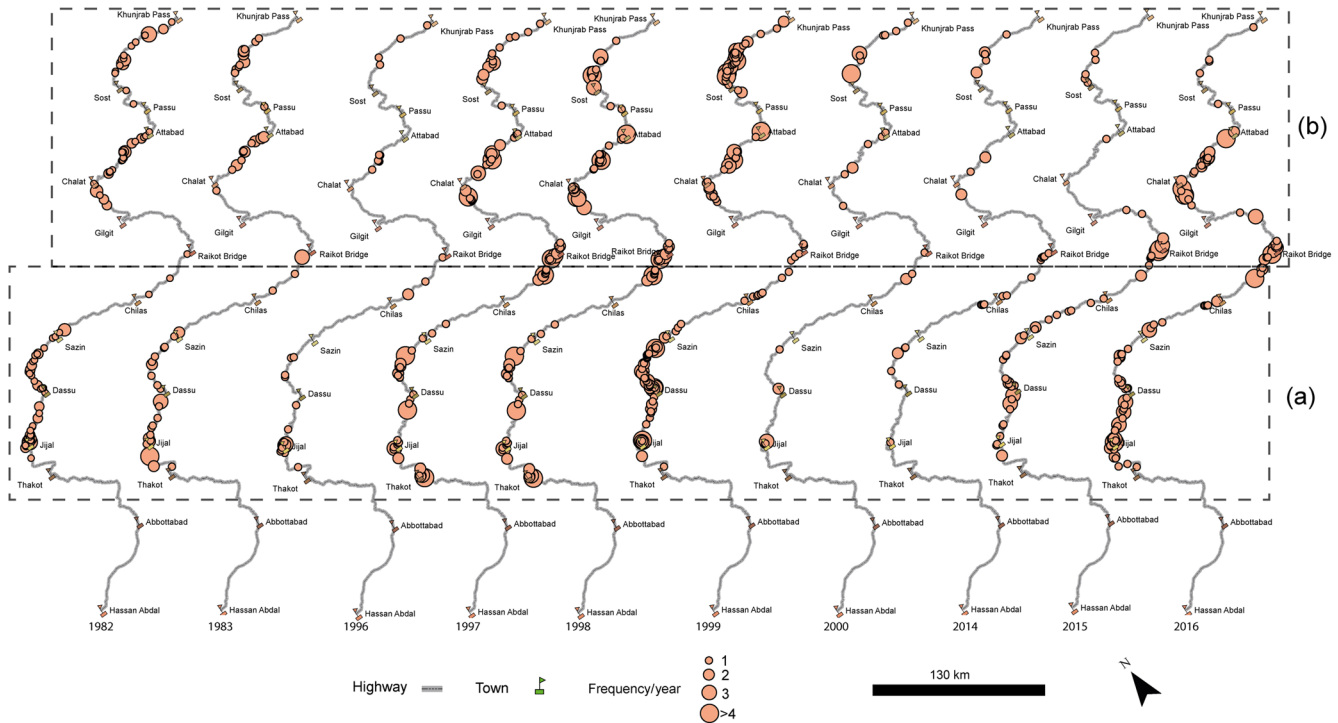


**Figure 6.** Temporal distribution of landslides along the highway: boxes (a) and (b) represent two problematic sections shown in Fig. 11.

landslide inventory map was then validated during a field campaign. Spatial analysis and validation of the final susceptibility map were performed by using these polygons. Due to the small scale of the inventory map, visibility of polygons was extremely low. Therefore, these polygons were then converted and displayed as points in the inventory map (Fig. 7).

**5.2 Field observation**

Locations of landslides, lithological contacts and faults were validated and supplemented during a field visit. In addition to locations, types, size, failure mechanisms and structural control of landslides were determined. Acquired data were further used to prepare a landslide inventory map within 2 km<sup>2</sup> around the highway.

**5.3 Remote sensing**

Geomorphological parameters (elevation, slope, aspect, curvature) and drainage were extracted from a DEM based on the Shuttle Radar Topography Mission (SRTM) (30 m × 30 m). Thematic layers were prepared and classified using the natural break method in GIS. Satellite images of Landsat 8 (19–21 November 2017) were acquired from the USGS web portal and then pre-processed by using QGIS 2.18’s semi-automatic classification plug-in (SCP), followed by supervised classification of composite images in GIS to prepare a land cover map.

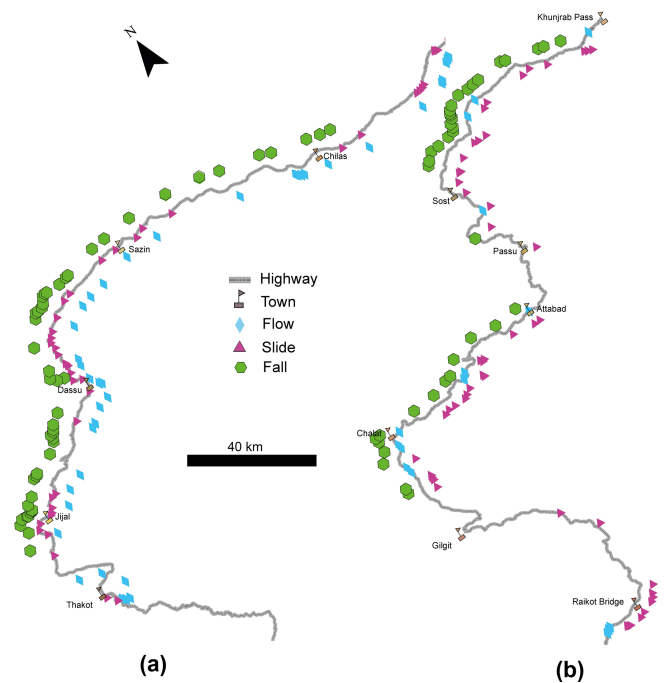


**Figure 7.** Types of mass movements along the highway. (a) Thakot to Raikot Bridge and (b) Raikot Bridge to Khunjerab Pass (locations shown in Fig. 6).

**Table 2.** Fundamental scale for pairwise comparisons (Saaty, 1987).

Intensity of importance	Explanation
1	Equal importance
2	Weak or slight
3	Moderate importance
4	Moderate plus
5	Strong importance
6	Strong plus
7	Very strong
8	Very very strong
9	Extreme importance

### Construction of thematic maps

Thematic layers of elevation, slope, aspect and curvature were prepared and classified using the natural break method in GIS. Drainage was extracted from the SRTM-based DEM by the Arc Hydro Tools. A buffer polygon of 300 m was created to measure distance around streams to form thematic layer of distance from drainage. Faults, lithology and seismic zones were digitized from previously published geological and seismic maps. Multiple ring buffer polygons of 500, 1000, 1500 and 2000 m around digitized faults were produced. Vector layers of distance from fault and drainage, lithology and seismic intensities were then rasterized. Annual rainfall data were interpolated to create a precipitation map and it was then combined with a previously published annual rainfall map of PMD. Thematic layer of land cover was produced from a land cover map.

### 5.4 Analytical hierarchy process

Analytical hierarchy process (AHP) is a multi-criteria decision making approach to prepare landslide susceptibility maps. It has been used by previous researchers to assign a weighting to landslide-controlling factors (Basharat et al., 2016; Kanwal et al., 2016; Shahabi and Hashim, 2015; Yalcin, 2008). It is based on the user's decision to weigh factors through their pairwise comparisons. Each factor is assigned a score (1–9) depending upon its relative importance, with increasing impact from 1 to 9 (Table 2, Saaty, 1990). The values assigned are based on spatial analysis of data, field observations and experience of the user. If the parameter on the  $x$  axis is more important than the one on the  $y$  axis, the value ranges between 1 and 9. Conversely, when the factor on the  $y$  axis is more important, the values are in reciprocals (1/2–1/9).

Consistency ratio (CR) is a tool to check and avoid inconsistencies and bias in the whole process of rating controlling parameters (Basharat et al., 2016; Kanwal et al., 2016; Komac, 2006; Pourghasemi and Rossi, 2017; Sarkar and Ka-

**Table 3.** Random consistency index (RI).

$n$	2	3	4	5	6	7	8	9	10
RI	0	0.58	0.9	1.12	1.24	1.32	1.41	1.45	1.51

nungo, 2004; Taherynia et al., 2014; Yalcin, 2008).

$$CR = CI/RI, \quad (1)$$

where CR is consistency ratio, CI is consistency index and RI is random index.

CI was calculated by using following equation:

$$CI = (\lambda_{\max} - n)/n - 1, \quad (2)$$

where  $\lambda_{\max}$  is the maximum eigenvalue of matrix and  $n$  is the number of controlling parameters involved (Zhou et al., 2016).

Saaty (1987) produced a table (Table 3) of random consistency index (RI) after calculation from 500 samples. Values of RI from this table and calculated CI were then compared to find CR.

The value of CR indicates the inconsistency in the expert's decision during weighing of the parameters. Values of CR lower than 0.1 prove the decision to be consistent, while values greater than 0.1 indicate inconsistency and suggest a revision of judgement. Subclasses in each factor were prioritized by using a pairwise comparison procedure (Table 4). Curvature and distance from drainage comprised of two and one classes, respectively. Therefore, influence of these subclasses was easily scaled without the AHP procedure. In the next step, each parameter was assigned a weighting on the completion of the procedure (Table 5). Value of CR in our study remained below 0.1, which proves comparisons and weighting criteria reliable, unbiased and consistent.

### 5.5 Weighted overlay method

Weighted overlay method (WOM) is a simple and direct tool of Arc GIS to produce a susceptibility maps (Bachri and Shresta, 2010; Intarawichian and Dasananda, 2010). Many researchers used WOM to produce landslide susceptibility map (Bachri and Shresta, 2010; Basharat et al., 2016; Intarawichian and Dasananda, 2010; Roslee et al., 2017; Shit et al., 2016). We used an overlay of raster layers of all controlling factors to prepare a susceptibility map. Raster layers of each controlling factor were reclassified and weighted according to their importance determined by AHP (Tables 4 and 5). The cumulative weight of all input layers was maintained at 100. All layers were combined by using the weighted overlay tool based on Eq. (3):

$$S = \frac{\sum W_i S_{ij}}{\sum W_i}, \quad (3)$$

where  $W_i$  is the weight of  $i$ th factor,  $S_{ij}$  represents subclass weight of  $j$ th factor and  $S$  is the spatial unit of the final map.

**Table 4.** Pairwise matrix and weights of factor subclasses.

Class	(1)	(2)	(3)	(4)	(5)	(6)	(7)	(8)	%	Importance
<b>Aspect</b>										
(1) North	1.00								2.59	2
(2) Northeast	2.00	1.00							5.89	3
(3) East	3.00	2.00	1.00						7.70	4
(4) Southeast	6.00	3.00	2.00	1.00					12.68	5
(5) South	7.00	4.00	2.00	1.00	1.00				16.71	6
(6) Southwest	8.00	4.00	3.00	2.00	2.00	1.00			21.95	7
(7) West	9.00	5.00	4.00	2.00	3.00	2.00	1.00		24.54	8
(8) Northwest	3.00	2.00	1.00	0.50	0.25	0.50	0.33	1.00	7.94	4
<b>Elevation (m)</b>										
(1) 432–1000	1.00								4.05	1
(2) 1000–2000	7.00	1.00							41.46	8
(3) 2000–3000	6.00	0.50	1.00						22.26	6
(4) 3000–4000	6.00	0.33	1.00	1.00					20.73	6
(5) 4000–4700	4.00	0.20	0.50	0.50	1.00				11.50	4
<b>Slope</b>										
(1) 0–15	1.00								3.92	1
(2) 15–30	3.00	1.00							11.00	4
(3) 30–45	9.00	4.00	1.00						41.46	9
(4) 45–65	8.00	3.00	0.50	1.00					30.83	6
(5) > 65	5.00	1.00	0.25	0.30	1.00				12.80	4
<b>Land cover</b>										
(1) Vegetation	1.00								9.68	2
(2) Water	0.33	1.00							4.75	1
(3) Snow	3.00	5.00	1.00						23.08	4
(4) Bare Rock/Soil	6.00	9.00	4.00	1.00					62.49	7
<b>Rainfall intensity (mm per year)</b>										
(1) 0–250	1.00								5.68	1
(2) 250–500	3.00	1.00							12.65	3
(3) 500–1000	5.00	3.00	1.00						27.35	5
(4) 1000–1500	8.00	5.00	3.00	1.00					60.00	9
<b>Lithology</b>										
(1) Group A (SI, AF, HF, KgB, MG, TaF)	2.00								4.52	1
(2) Group B (BeG, SC, TeF)	4.00	1.00							8.14	2
(3) Group C (KoB, KaB, CC, GilF, GJ)	6.00	2.00	1.00						14.83	4
(4) Group D (KA, GirF, KF, RPV, SC)	8.00	3.00	2.00	1.00					26.02	6
(5) Group E (Qu, JC, OM, MS, PS, NPG, BaG)	4.00	5.00	4.00	2.00	1.00				46.49	9
<b>Seismic intensity</b>										
(1) I–III	1.00								3.74	2
(2) IV–V	3.00	1.00							7.63	3
(3) V–VI	5.00	3.00	1.00						14.22	6
(4) VII–VIII	7.00	5.00	3.00	1.00					29.77	8
(5) IX–X	8.00	6.00	4.00	2.00	1.00				44.64	9
<b>Distance from a fault (m)</b>										
(1) 0–500	1.00								50.50	9
(2) 501–1000	0.50	1.00							27.04	7
(3) 1001–1500	0.25	0.50	1.00						15.30	5
(4) 1501–2000	0.20	0.25	0.33	1.00					7.15	4

**Table 5.** Pairwise matrix and weights of all controlling parameters.

Controlling factors	Aspect	Elevation	Fault	Lithology	Land cover	Distance from drainage	Rainfall intensity	Slope	Curvature	Seismicity	Weight
Aspect	1										1.77
Elevation	3	1									3.05
Distance from fault	9	7	1								23.28
Lithology	6	5	1/3	1							10.28
Land cover	4	3	1/4	1/3	1						7.04
Distance from drainage	6	5	1/3	1	2	1					8.90
Rainfall intensity	5	4	1/4	1/2	2	1/2	1				7.08
Slope	9	7	1	3	5	3	4	1			23.74
Curvature	1	1/3	1/9	1/6	1/5	1/5	1/5	1/7	1		1.82
Seismicity	7	5	1/3	1	4	2	3	1/3	7	1	13.03

The completion of this process resulted in the ultimate production of a landslide susceptibility map of the highway.

## 6 Results

### 6.1 Landslides along the KKH

A total 261 landslides were used to prepare the map (Table 6). Broadly, we grouped these into shallow and deep-seated landslides (rock avalanches). Shallow landslides were further divided into slides, falls and flows based on the simplified version of Varnes (1978). Four sections (Table 6) are characterized by a large number of landslides during heavy rainfall and snowmelt. Highway blockage and traffic interruption in these sections is a regular phenomenon. Presence of a large number of rock/debris falls (37) in Jijal–Dassu section is due to steep topography formed by deep river incision in ultramafics (Jijal Complex), amphibolites (Kamila amphibolites) and gabbro-norites (Chilas Complex) of Kohistan Island Arc, whereas stress release joints with short persistence in Sazin–Chilas section are responsible for huge boulder falls ( $> 6 \text{ m}^3$ ). A large number of slides (rock, debris and mud) and flows (debris and mud) in large old landslide deposits characterize the Raikot Bridge section. Hunza valley section is dominated by slides (rock, debris and mud) in highly sheared rock mass and falls (rock and debris) in over-steepened parts of the valley. Steady flow of traffic along the highest section (Sost–Khunjerab Pass) of the highway is a major problem due to seasonally influenced falls and slides. This section has a large number of large landslides (16), which dammed the Hunza and Khunjerab rivers in the past.

### 6.2 Causative factors and spatial distribution analysis

Geological, morphological, seismo-tectonic, topographic and climatic factors are generally considered landslide-controlling parameters (Kamp et al., 2008). The following 10 causative factors were considered for preparation of the map: lithology, distance from faults, seismicity, elevation, slope,

aspect, curvature, land cover, rainfall intensity and distance from drainage. Size and distribution of the landslides varies locally, depending on the values of the parameters mentioned above. Thus, the creation of an accurate and precise GIS-based landslide susceptibility map is entirely dependent on the availability of data related to controlling factors (Ayalew et al., 2004). Rockslides, debris slides, rock avalanches, rock fall, toppling, wedging, mudflows and debris flows are important landslide processes along the KKH.

#### 6.2.1 Lithology

Time and type of slope failure is determined by the slope-building lithology. Each lithology is unique in terms of response to stresses and therefore features a particular susceptibility to potential slope failure (Vallejo and Ferrer, 2011). The KKH traverses a great variety of lithologies comprising sedimentary, igneous and metamorphic rocks. According to spatial analysis, Quaternary deposits, the Jijal Complex and the Misgar slates exhibit the highest numbers of mass movement events (Fig. 8f).

#### 6.2.2 Distance from faults

The main mantle thrust (MMT), the Kamila Jal shear zone (KJSZ), the Kamila strike-slip fault (KSF), the Raikot Fault, the main Karakoram thrust (MKT) and the Karakoram Fault are important structural features in close proximity to the highway (Fig. 4). Landslides are concentrated along these active faults where rock mass is highly deformed (Ali et al., 2017). The fact that 54 % of mapped landslides were found within a maximum distance of 1 km from these faults, while 69 % were found within a 2 km range, impressively substantiates the postulated strong control of structural features (Fig. 8e).

#### 6.2.3 Geomorphologic factors

Slope angle is an important geomorphic factor responsible for initiation of slope movements (Lee et al., 2004) to be considered for preparation of landslide susceptibility maps.

Table 6. Types of landslides along the KKH.

Section	Rock falls	Flows (debris, mud)	Shallow landslides	Deep-seated landslides/ rock avalanches
Jijal–Dassu section (91 km)	37	17	19	1
Sazin–Chilas section (90 km)	10	9	7	4
Raikot Bridge section (49 km)	5	8	15	5
Hunza Valley section (76 km)	13	6	15	10
Sost–Khunjerab valley section (86 km)	22	8	16	16
Rest of the highway (321 km)	2	2	14	0
Total	89	50	86	36

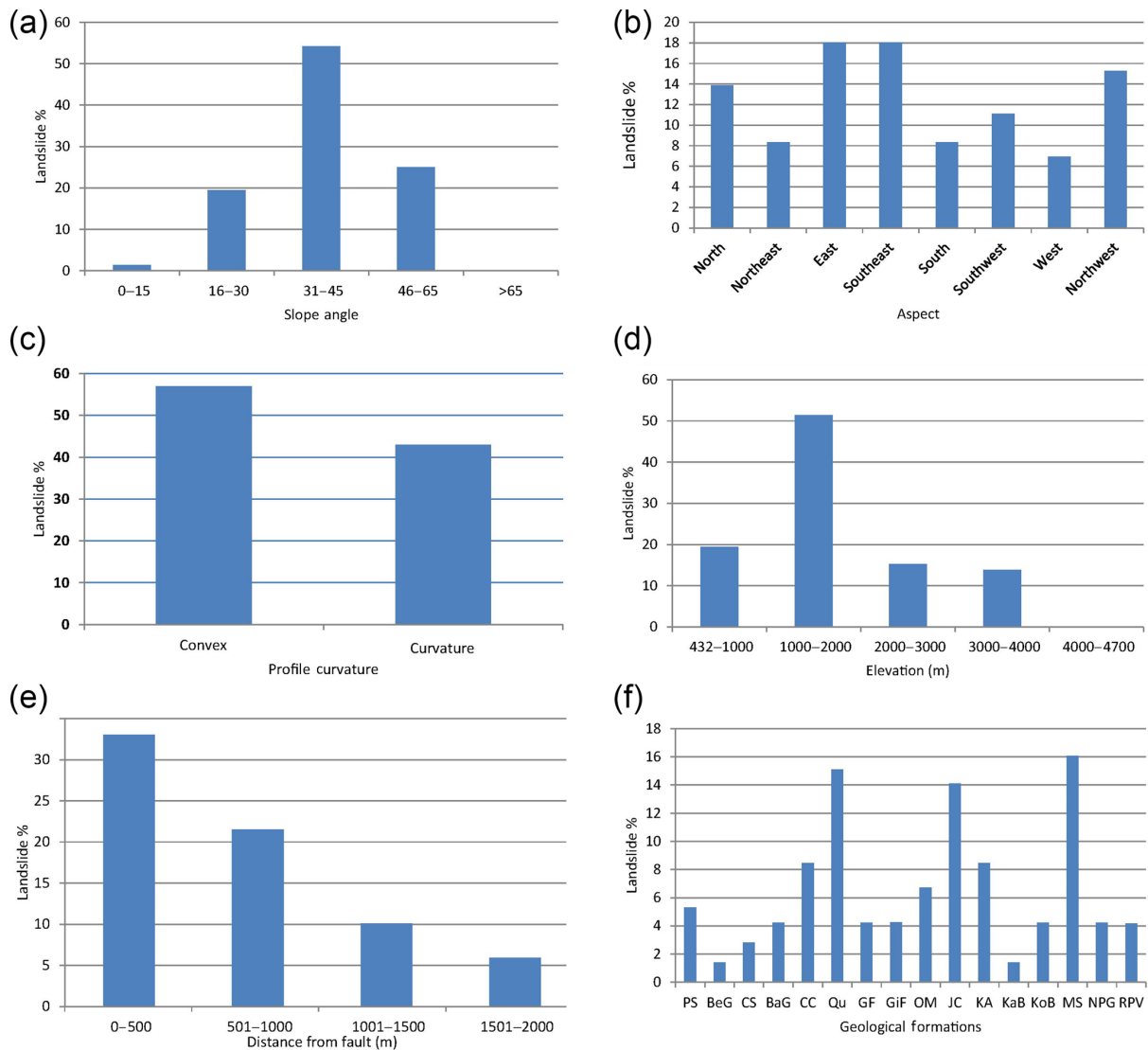


Figure 8. Frequency distribution histograms of controlling parameters: (a) slope angle, (b) aspect, (c) profile curvature, (d) elevation, (e) distance from fault, (f) geological formation (abbreviations explained in Fig. 5). BaG: Baltit Group, BG: Besham Group, Cc:Chilas Complex, GilF: Gilgit Formation, GirF: Gircha Formation, JC: Jijal Complex, KA: Kamila amphibolite, KaB: Karakoram batholith, KoB: Kohistan batholith, MS: Misgar slates, NPG: Nanga Parbat granitic gneisses, OM: Ophiolitic Melange, PS: Passu slates, Qu: Quaternary, RpV: Raka-poshi volcanics, TF: Theilichi Formation, F: fault, TF: thrust fault, MMT: main mantle thrust, KJS: Kamila Jal shear zone, KSF: Kamila strike–slip fault, RF: Raikot Fault, KF: Karakoram Fault, MKT: main Karakoram thrust.

Steep slopes are more susceptible to failure as compared to gentle ones. The study area demonstrates variation in topography ranging from steep to gentle slopes, high plains to narrow gorges and high cliffs. Slope steepness in the area has been divided into five classes. Division of slope steepness into classes was based on statistical analysis. Different classes were tried but we found this division to be better in our study area. More than 50 % of landslides occurred in class III (30–45°) areas, whereas the least landslide events (2 %) occurred in class I and class V (0–15 and > 65°) areas (Fig. 8a). In addition to slope and elevation, aspect and curvature were also considered important factors for preparation of the landslide susceptibility map. However, in our area these parameters seem to have a reduced influence on landslide occurrence (Fig. 8b, c, d).

#### 6.2.4 Hydrology

The proximity of streams has been considered for the preparation of landslide susceptibility maps by many researchers (Akgun et al., 2008; Basharat et al., 2016; Kanwal et al., 2016; Wang et al., 2015). In our study area, many small tributaries feed main rivers (Indus and Hunza). During monsoon season and after heavy precipitation events, these streams exhibit high-energy flows and large discharge, and are the main source of mud and debris flows. Heavy precipitation during the monsoon and the westerlies triggers many landslides by increasing pore water pressure in unconsolidated sediments. Annual precipitation map of the area was prepared based on the Pakistan Meteorological Department (PMD) data (Fig. 3a). A strong association between precipitation and mass movements along the highway has been found (Fig. 3b) (Ali et al., 2017). Peaks in mass movement curve is clearly synchronizing with high precipitation in respective months (Fig. 3b). A large number of landslides along the KKH occurred in 1999 leading to traffic blockade. The precipitation map was then overlaid to landslide events (1999). A large number of landslide events were found south of Sazin with annual precipitation more than 1000 mm per year. The section of the KKH east of Sazin contained comparatively less landslides due to its location in semi-arid to arid climate zones (> 250 mm per year). Similar control of rainfall over landslide events has also been found in the rest of the KKH.

#### 6.2.5 Land cover

Variations in land cover control the spatial distribution of landslides along with other conditioning parameters (lithology, seismology, slope geometry) (Malek et al., 2015). Changes in land cover influence the hydrological condition of the slopes, leading to slope instability. Generally, vegetation tends to resist the erosion process, whereas bare rock or soil is more susceptible to slope failure (Reichenbach et al., 2014). Restrepo and Alvarez (2006) found a strong relationship between land use and landslide events. Previous

experts used a variety of software and techniques to produce a land cover map from satellite imagery. Many of them used the maximum likelihood (ML) supervised classification tool (Ahmad and Quegan, 2012; Butt et al., 2015; Escape et al., 2013; Pourghasemi et al., 2012; Reis, 2008; Rwanga and Ndambuki, 2017; Ulbricht et al., 1993). All land cover maps produced by this technique had an accuracy of more than 80 %. Optical images of Landsat 8 (19–21 November 2017) were downloaded from the USGS database. These images were then orthorectified and atmospherically corrected by using the semi-automatic classification plug-in (SCP) of QGIS 2.18. Composite images were classified by using GIS's maximum likelihood (ML) supervised classification tool. Training data and spectral signature file were created to represent four uniform classes (vegetation, water bodies, snow and bare rock/soil). The produced map was divided into four classes: vegetation, water bodies, snow and bare rock/soil. The final land cover map was assessed using the confusion matrix method. Randomly distributed test pixels for each class were taken on the same image that had previously been classified. The accuracy of the land cover map added up to 87 %. Due to variations in the mountain ecosystem from Hassan Abdal to Khunjerab Pass, the KKH is surrounded by vegetation, bare rock/soil, water bodies and ice/snow covered slopes. The section of the highway between Hassan Abdal and Thakot is heavily vegetated due to considerable mean annual rainfall. From Thakot to Sazin, slopes are sparsely vegetated. From Sazin onward, barren rock slopes characterize the area.

In the end, spatial density analysis was performed to check the influence of land cover changes on landslide events. Results revealed that more than 50 % of landslides were located in bare rock/soil category, whereas vegetation and snow-covered areas contain 23 % each. Processed satellite images were captured at the start of the winter season (19–21 November 2016). Most of the slopes in north of Gilgit were covered by snow at this specific time. It justifies the presence of 23 % landslides in the snow/glacial ice class.

#### 6.3 Landslide susceptibility map

The produced landslide susceptibility map was classified into four classes: low susceptibility, moderate susceptibility, high susceptibility and very high susceptibility (Figs. 9 and 10). Nine susceptibility levels were converted into four levels. Each has an interval of two except for the high susceptibility level, which contains three susceptibility levels: 5, 6 and 7. It was done to distinguish the locations that are more hazardous.

Areas of 49.9 % and 10.4 % of the classified map, respectively, belong to the high susceptibility and very high susceptibility classes, particularly owing to the presence of active faults, seismic zones and steep slopes (Table 7). Percentages of 34.1 % and 5.4 % of the highway fall into intermediate and low susceptibility areas, respectively.

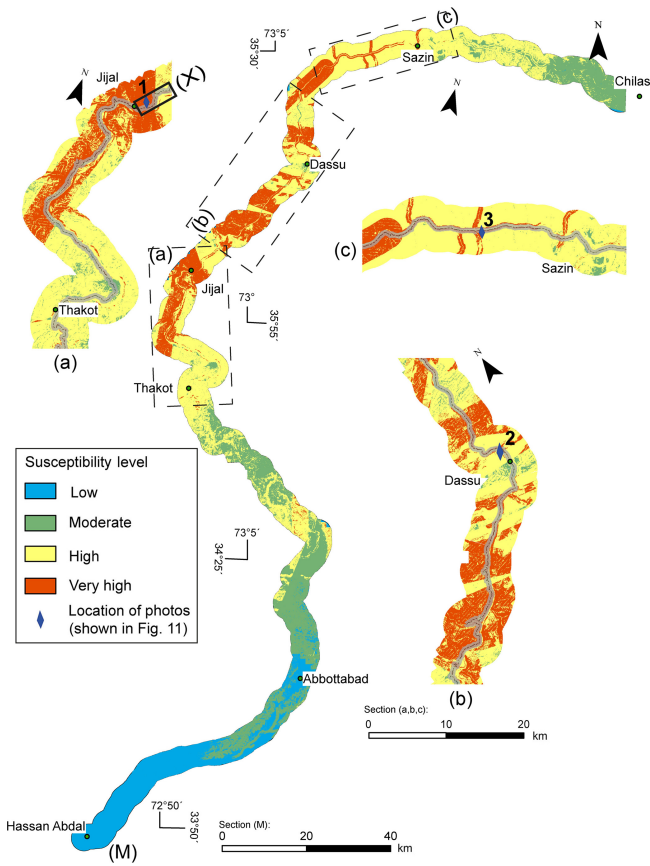


**Figure 9.** Landslide susceptibility map (Abbottabad–Chilas): (a) Jijal section (area in box “X” is shown in Fig. 15), (b) Dassu section and (c) Sazin section.

**Table 7.** Area of susceptibility classes.

Classes	Area (%)
Low risk	5.4
Intermediate risk	34.1
High risk	49.9
Very high risk	10.4

For clarity and spacing, the final version of the map was divided into two parts: (1) Hassan Abdal–Chilas section and (2) Chilas–Khunjerab Pass section (Figs. 9 and 10). The highway section 1 until Thakot is characterized by broad valleys and gentle slopes covered by vegetation and therefore falls into the low to intermediate susceptibility zones (Fig. 9). Contrastingly, the following section north of Thakot, particularly close to Jijal, lies in high and very high susceptibility zones (Fig. 9a). Threats arise from the presence of the southern suture (MMT), poor rock mass quality, the active IKSZ and steep slopes. In the section from Pattan to Sazin, more than half of the highway is at high susceptibility and very high susceptibility (Fig. 9b and c). This is because multi-

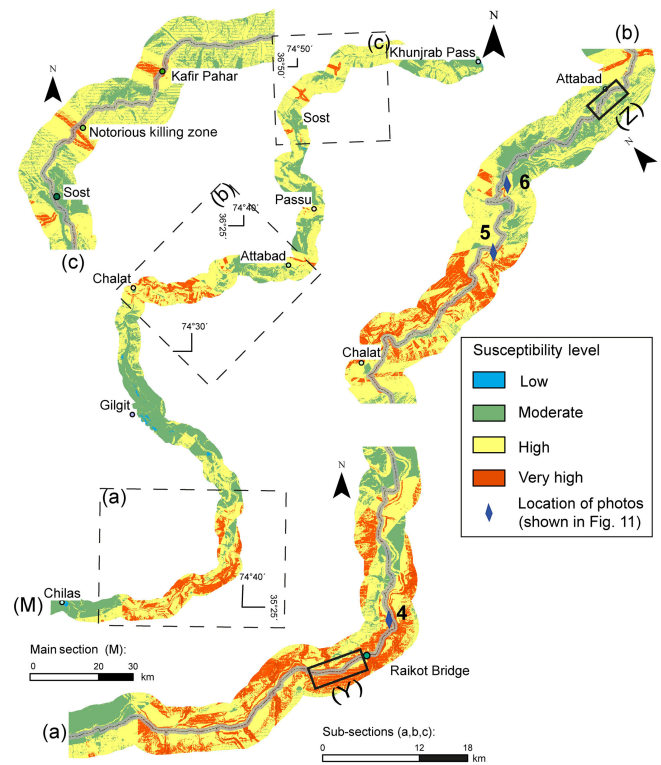


**Figure 10.** Landslide susceptibility map (Chilas–Khunjerab Pass): (a) Raikot Bridge section (box “Y” is shown in Fig. 14), (b) Attabad section (box “Z” is shown in Fig. 15) and (c) Sost section.

ple shear zones (KJS) cross the highway between Pattan and Dassu and the surroundings of Sazin fall into the reach of the Kamila strike–slip fault (KSF) and the active HSZ (Fig. 9c). Two locations close to drainage features (Samar and Harbon Nala) near Sazin (Fig. 9c) also fall into the very high susceptibility zone.

The second section starts in Chilas and ends at the Khunjerab Pass (Chinese border). Some parts of the highway were found at very high susceptibility (Fig. 10). The Raikot Bridge section is the most dangerous part of the highway as it lies directly over the active Raikot Fault (RF) and passes through RSSZ. Steep slopes and continuous erosion of slope toes by the Indus River are aggravating the situation (Fig. 10a). Due to the presence of the northern suture (MKT), loose glacial deposits and steep slopes in the Hunza section, some locations of the highway are declared very high susceptibility zones (Fig. 10b). Also, north of Sost, two locations (Kafir Pahar and notorious killing zone) were found in very high susceptibility zones (Fig. 10c).

#### 6.4 Accuracy assessment

Accuracy assessment of the map is an essential component of the whole process. In the past, different statistical techniques have been employed to check the predictive ability of a landslide susceptibility map: predication rate curve



**Figure 11.** Example of landslide events (Ali et al., 2017) (locations of the photos are given in Figs. 9 and 10).

(PRC), landslide density analysis (LDA), receiver operating curve (ROC) and area under curve (AUC) (Deng et al., 2017). ROC is a better choice than other techniques as it is threshold independent and measures both accuracy and error rate (Fawcett, 2006; Vakhshoori and Zare, 2018). Multiple researchers used ROC for validation of produced maps (Ahmed, 2015; Basharat et al., 2016; Lee, 2005; Zhou et al., 2016). In this study, we also used ROC and LDA to estimate the predictive accuracy of the map.

In the first step, map classes were compared with landslide densities in their respective classes. Spatial analysis of the map and landslide events was performed on GIS using the tabulate area tool. According to the obtained results, most of the landslide events were found in high and very high susceptibility areas and very few landslides were present in moderate and low susceptibility zones (Table 8). These statistics confirm a strong connection between susceptibility zonation and landslide events. Thus, this assessment indicates an adequate accuracy of the map.

**Table 8.** Areas of susceptibility level of map and observed landslides.

Susceptibility level	Area (km <sup>2</sup> )	Landslides
1	1.3	0
2	342.1	0
3	627.2	0
4	1517.1	1
5	1819.0	8
6	1316.1	29
7	585.3	20
8	67.4	13
9	0.2	1

In the second step, we used ROC for validation and accuracy assessment of the map, following the example of previous studies (Ahmed, 2015; Basharat et al., 2016; Brenning, 2005; Deng et al., 2017; Pradhan et al., 2010; Shahabi and



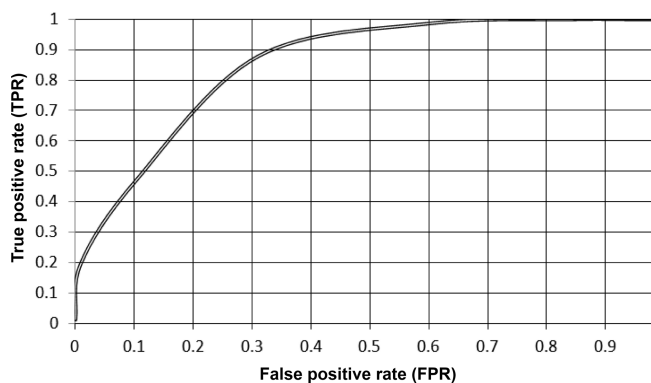


**Figure 12.** ROC-based accuracy assessment of the landslide susceptibility map.

Hashim, 2015). ROC is the product of a graphical plot opposing true positive rate (TPR) and false positive rate (FPR) (Fig. 12). TPR indicates the correctly predicted events and is plotted on the  $y$  axis while FPR indicates falsely predicted events, and is plotted the  $x$  axis. Area under curve (AUC) in a graphical plot explains the efficiency of the model. AUC may range from 0.5 to 1 in different cases depending on the accuracy of the model. A value close to 0.5 indicates random results while values close to 1 indicate a perfect model (Ahmed, 2015). In this study, we used 72 landslide locations to validate the final version of the map. AUC was found 0.72 indicating a reputable accuracy (72 %) of the map (Basharat et al., 2016; Deng et al., 2017).

## 7 Discussion

In this study, the AHP-based weighted overlay technique was used to produce landslide susceptibility maps along the KKH. Ten landslide controlling factors were considered for production of landslide susceptibility maps. Review of previous published articles helped us to finalize causative factors responsible for the occurrence of landslides. Afterwards, spatial analysis was performed to prioritize and rate these parameters. The clustering of landslides in active fault and shear zones indicate their strong control. These tectonic features resulted in highly fractured and jointed rock masses, highly susceptible to failure. Slope gradient and distance from a fault were considered basic conditions for slope instability and rated as the most important factor. Major seismic events in active seismic zones in close vicinity of the highway triggered landslides in the past. Some lithologies (slates, shales, Quaternary sediments) exhibit low shear strength and make slopes susceptible to failure. Therefore, seismicity and lithology are rated high but less important than slope gradient. Torrential rainfall in the monsoon and westerlies seasons triggers landslides and was taken into account. However, its influence decreases north of Gilgit, where the cumulative effect of ice melt with rise in temperature and rainfall cause

landslides. Other geomorphic factors (elevation, aspect, curvature) were rated low because of their poor association with landslide events.

Quality of the data sets directly influences the quality of results (Fressard et al., 2014). Landslide inventory is the most important and basic data set among them. Inaccuracies regarding location and recent activity of landslides adversely affects the accuracy of the final map. We prepared and used landslide inventory by using satellite imagery, landslide activity logs encompassing over 10 years (Fig. 6) and then field surveys to validate locations and extent of landslides. The combination of all these aspects has led to an error-free inventory. We used geological maps (1 : 50 000 and 1 : 250 000; Khan et al., 2000) explaining lithological variations within formation and also having both regional and local faults. Lithological contacts and location of faults and shear zones were verified during a field visit. Seismic intensities and PGA (peak ground acceleration) values were derived from the shake map of instrumental earthquakes (USGS). Rainfall data of six uniformly distributed weather stations was used to prepare annual rainfall map. Land cover map was prepared from Landsat 8 optical imagery having 30 m resolution. Images captured in November 2017 (before winter) were used to have snow free slopes along the KKH. Keeping in mind that the objective was to produce landslide susceptibility map along the highway, four classes (vegetation, water bodies, snow and bare rock/soil) were derived and temporal variability in land use was not considered. In this study, quality of the data sets was comparatively better than previously used.

Many authors used an AHP-based model to prepare susceptibility maps (Ahmed, 2015; Arizapa et al., 2015; Bachri and Shresta, 2010; Basharat et al., 2016; Intarawichian and Dasananda, 2010; Kamp et al., 2008; Komac, 2006; Park et al., 2013; Pourghasemi et al., 2016, 2012; Pourghasemi and Rossi, 2017; Rahim et al., 2018; Rozos et al., 2011; Shahabi and Hashim, 2015; Yalcin, 2008). Comparison of AHP-based models with other models in some studies (Pourghasemi et al., 2012, 2016; Pourghasemi and Rossi, 2017; Shahabi and Hashim, 2015; Yalcin, 2008) proved the former to be more accurate and precise. Accuracy of the produced map in this study is 72 % which is satisfactory but slightly less than previous studies (Basharat et al., 2016; Kanwal et al., 2016; Pourghasemi et al., 2012; Pourghasemi and Rossi, 2017; Shahabi and Hashim, 2015; Yalcin, 2008). AHP is a simple and easy way to rate different parameters consistently. Value of CR remained below 0.10 for each case, indicating appropriate and reliable weighting criteria. However, the AHP-based model has been criticized due to its expert-opinion-based subjective approach. Therefore, we performed spatial analysis to rate all controlling parameters to minimize chances of errors related to cognitive limitations of the expert. Further, due to low spatial resolution of the DEM (30 m  $\times$  30 m), some cut slopes along the KKH were neglected. Rating system introduced in this study may not fit into any other re-

gions due to variations in geological, seismic, hydrological and other controlling parameters. Lastly, change in existing conditions (undercutting of landslide toes for highway expansion) of landslide controlling parameters may change present susceptibility along the highway.

## 7.1 Case study

To supplement results and finalize the landslide susceptibility map, three sub-sections were discussed: Jijal sub-section, Raikot Bridge sub-section and Attabad sub-section.

### 7.1.1 Jijal sub-section

Part of the highway north of Jijal town lies in a zone of very high susceptibility (box b of Fig. 9a). It comprises highly fragmented ultramafic rocks of the Jijal Complex. Due to its position in the hanging wall of MMT, it is highly jointed and locally sheared. The area is seismically active and located just 3 km away from the epicentre of the Pattan Earthquake on 28 December, 1974 ( $M = 6.2$ ,  $D = 22$  km). The seismic intensity (Modified Mercalli Intensity Scale) of this event along this part of the highway reached VIII (Ambraseys et al., 1981). Furthermore, the  $S$  of this area is seismically very active (Fig. 4c). During the catastrophic October 2005 Kashmir Earthquake ( $M = 7.6$ ), some landslides were reactivated, leading to a closure of the highway. Topography in this part is steep, with slope angles ranging between 40 and 70°. The area lies in the monsoon region where average annual rainfall exceeds 1000 mm. The dotted yellow lines (Fig. 13a) indicate a big catchment area (1.34 km<sup>2</sup>), capable of collecting large amounts of water during rainfall, leading to debris flows and debris slides in sheared and highly fragmented rock masses. Rock and debris falls are further promoted by clayey soils that form in joint apertures as a result of serpentinization. Due to heavy rainfall (617 mm) in March and April 2016, a large number of landslides were reactivated leading to blockage of the highway for 2 weeks. All these factors (closeness to fault, high seismicity, fragmented rock mass, heavy rainfall, steep topography) are responsible for the very high landslide susceptibility in this area.

### 7.1.2 Raikot Bridge sub-section

Stability of the highway is a challenge for geologists, civil engineers and highway authorities. The highway subsidence due to river undercutting and presence of the active Raikot Fault (RF) is a continuous threat. Hot water springs and a shear zone (ca. 125 m wide) indicate the presence of RF. It marks the boundary between Precambrian granitic gneisses of the Indian plate and batholiths and gabbro-norites of the Kohistan Island Arc. RF is responsible for shallow seismicity along the highway (Fig. 4c). Seismic intensity (Modified Mercalli Intensity Scale) in this part reaches VI. The rock mass is highly jointed and sheared due to the presence of the fault. Furthermore, the continuous seepage from

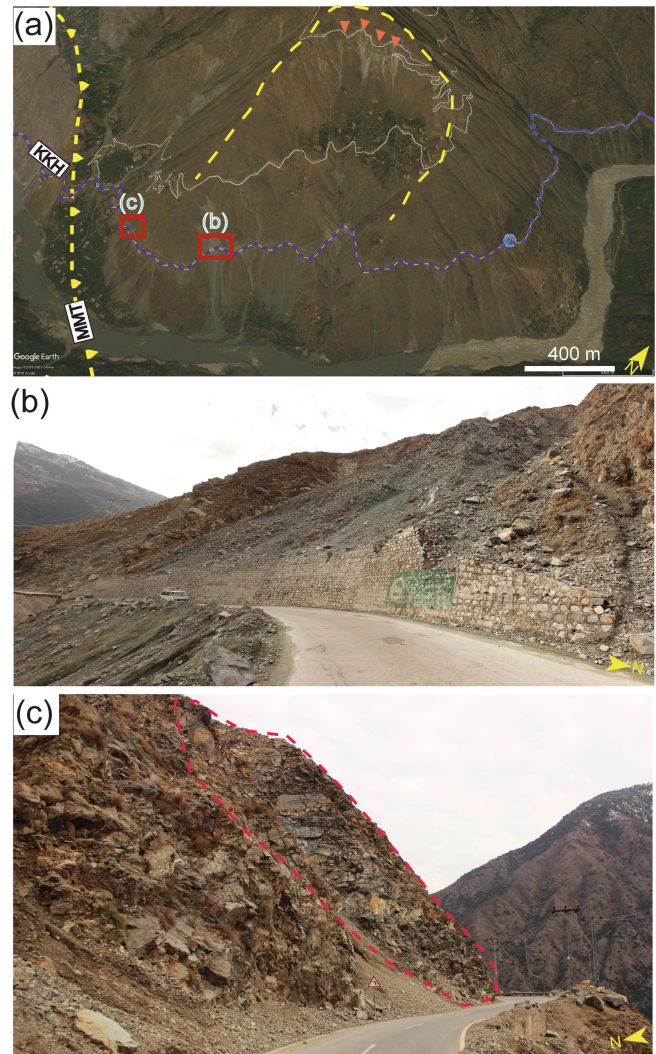


**Figure 13.** Very high landslide susceptibility along the KKH near Jijal (Google Earth, 2017a, Bing Maps) (for location see Box “X” in Fig. 12a). (a) Overview of 7.5 km long small section of the highway northeast of Jijal: dotted black line represents MMT; dotted yellow line marks the boundary of catchment area (1.34 km<sup>2</sup>); pink arrows show ongoing rock/debris falls, which travel downslope along with water during heavy rainfall; gully erosion is prominent. (b) Famous “Shaitan Pari Slide” with partially damaged retaining wall. Reactivation of this slide is mostly during heavy rainfall. (c) Highly jointed rock mass is highly susceptible to rock/debris fall.

hot water springs results in weathering and a lower shear strength of the rock mass. In the past, two large landslides dammed the Indus River (Fig. 14a). Deposits of these landslides contain retrogressive slope movements and debris flows (Fig. 14a). Landslide damming had several effects on terraces and slopes, including the deposition of alluvial and lake deposits. In addition to this, continuous rockfall is adding large quantities of debris to the slopes. Topographically, this section is also very steep. Climatically, it lies in a semi-arid to arid zone with an average annual rainfall of 0–

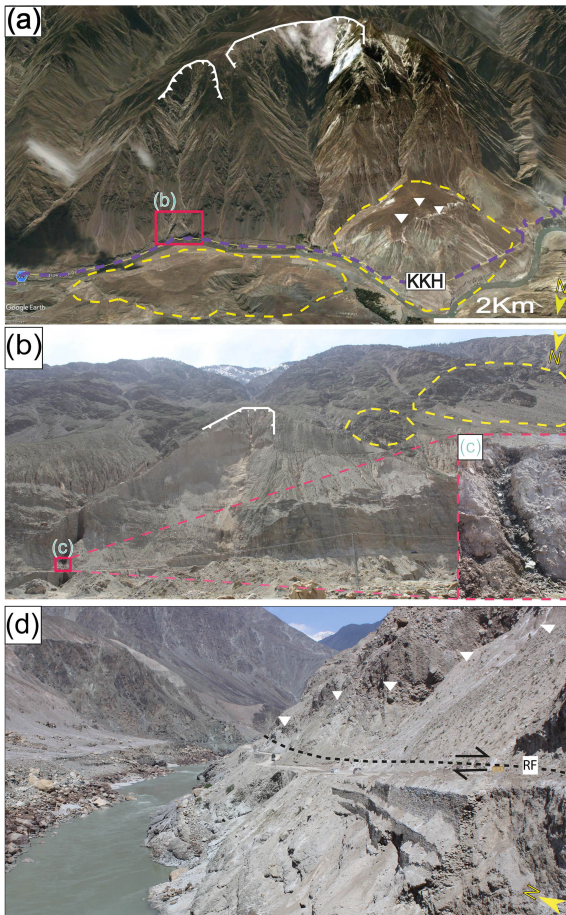


**Figure 14.** Very high landslide susceptibility near Raikot Bridge (Google Earth, 2017b, Bing Maps) (for location see Box “Y” in Fig. 13b). (a) Overview of 13.4 km long small section west of the Raikot Bridge: white lines represent main scarps of large landslides/rock avalanches, which dammed the Indus River in the past; dotted yellow circles represent deposits of these old landslides; white arrows are showing sagging in landslide deposit which is due to retrogressive rotational failure. (b) White line represents scarp of shallow landslide in alluvial deposits (area in red box of panel a); area in dotted yellow circles represents ongoing rock/debris fall supplying scree/talus for debris flow during rainy season. (c) One of the hot water springs (90–96 °C) along the highway in this section. (d) Another view of small section: white arrows are marking upper limit of the shear zone (ca. 125 m wide); dotted black representing active RF marked along shear zone; overhangs above and river erosion below the highway makes this section highly susceptible to slope failures.

250 mm. Rainfall, however, is restricted to a couple of events per year. On 3 and 4 April, 2016, 105 mm rainfall reactivated debris flows and slides. The prevailing circumstances make this part of the highway highly susceptible to landslides.

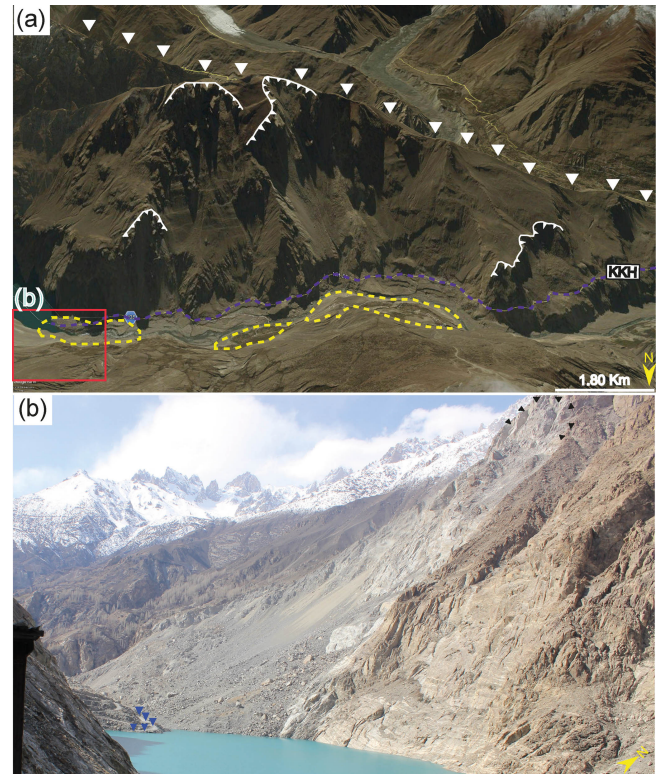


**Figure 15.** High landslide susceptibility along the highway in Hunza Valley (Google Earth, 2017c, Bing Maps) (for location see Box “Z” in Fig. 13b). (a) Overview of 11 km long small section west of the Attabad Lake: white lines are representing the main scarps of old large landslides/rock avalanches which dammed the Hunza River in past; dotted yellow circles represent deposits of these old landslides; white arrows are showing location of local fault. (b) Attabad landslide (in red box of panel a); blue arrows are showing the highway submerged in lake water.

### 7.1.3 Attabad sub-section

Hunza section has a variety of slope failures depending upon prevailing geological and climatic conditions. However, the area shown in Fig. 15 is characterized by falls (rock, debris) and some slides (rock, debris). Historically, large landslides (1858, 1980, and 2010) dammed Hunza River in this part (Fig. 15a). The area is characterized by highly weathered and jointed granodiorites, orthogneisses and pegmatitic veins of the Kohistan Batholith. The orientation of joints (dipping in the same direction as the slope) has an adverse impact on slope stability. The area is located in the hanging wall of MKT, the main fault in this region, and a local fault exists in the close vicinity (Fig. 15a). Past earthquakes (Astore, 2002;  $M = 6.3$  and Muzaffarabad, 2005;  $M = 7.6$ ) produced ground shaking intensity of up to V–VI (Modified Mercalli Intensity Scale). Climatically, the valley floor is part of a semi-arid zone (250–500 mm per year) while the higher slopes and peaks (> 5000 m) receive precipitation of

$\geq 1000$  mm per year. Therefore, the area is sparsely vegetated. Rainfall coupled with snowmelt in early spring reactivates old landslides (Ali et al., 2017). Undercutting of landslide toes by Hunza River below the highway and rock/debris fall upslope are major concerns in this section. All of the abovementioned circumstances yield a high landslide susceptibility for this section (Fig. 11).

## 8 Conclusions

A set of landslide susceptibility maps of the KKH (CPEC) was prepared using GIS involving multiple techniques: literature review, remote sensing and field surveys. Ten controlling parameters (lithology, seismicity, rainfall intensity, distance from fault, elevation, slope angle, aspect, curvature, land cover and hydrology) were considered of which each one was assigned a numerical weight using AHP. Thematic layers of these parameters were then overlaid using the WOL tool of GIS. Four different classes of landslide susceptibility were then applied to the final map: low susceptibility, moderate susceptibility, high susceptibility and very high Susceptibility. Percentages of 10 % and 50 % of the highway were found in very high and high susceptibility zones, respectively. Active faults (MMT, KJS, KSF, RF, MKT, KF), seismic zones (IKSZ, HSZ, RSSZ) and steep slopes are responsible for the associated susceptibility in these areas. The highway is characterized by a variety of mass movements: rockfall, debris fall, rockslide, debris slide, debris flows and mudflows. The threatened sections are especially unstable in monsoon and westerlies seasons every year. Altogether, a detailed investigation is inevitable to enable hazard-free and safe travelling. About 40 % of the highway lies in low and moderate susceptibility zones, which remain almost stable throughout the year. The highway sections from Hassan Abdal to Thakot, near Chilas, Gilgit and Sost fall into these moderate and low susceptibility zones and are quite stable due to their course in broad U-shaped valleys with gentle slopes. Although the part of the highway between Hassan Abdal and Thakot receives heavy precipitation in the monsoon season, the area is stable owing to a mature geomorphology. Due to closeness with MMT, higher seismic intensity and steep topography, the KKH near Raikot Bridge and Jijal was found to be at very high risk. Furthermore, extreme weather conditions, highly shattered and weathered rock masses, active faults and long, steep slopes are responsible for very high and high susceptibility around Attabad, notorious killing zone and Kafir Pahar sites. According to results, active faults, slope gradient, seismicity and lithology have a strong influence on landslide events along the highway. In the final step, the predictive accuracy of the map was determined by using LDA and ROC. The accuracy of the map was rated to a satisfactory 72 %, which is suitable for mitigation planning.

*Data availability.* Data cannot be shared at this stage as authors are currently analysing for further work.

*Author contributions.* SA constructed an idea, planned methodology, interpreted results, and then reached conclusions. KR supervised the whole process and provided personal, environmental, and financial support for the research work. PB and RH took responsibility for literature review and assisted SA in finalising the whole paper and in the end critically reviewed the paper before submission.

*Competing interests.* The authors declare that they have no conflict of interest.

*Special issue statement.* This article is part of the special issue “Landslide–road network interactions”. It is not associated with a conference.

*Acknowledgements.* We would like to thank the Higher Education Commission (HEC) of Pakistan and the German Academic Exchange Service (DAAD) for financial support for the research project. Also, we thank Paolo Tarolli, anonymous referees, Muhammad Basharat and Aram Fathian Baneh for their valuable suggestions. Further, we would like acknowledge the Frontier Works Organization (FWO) and the Pakistan Meteorological Department for provision of data for analysis.

*Review statement.* This paper was edited by Paolo Tarolli and reviewed by Ananta Man Singh Pradhan and four anonymous referees.

## References

- Ahmad, A. and Quegan, S.: Analysis of Maximum Likelihood Classification on Multispectral Data, *Appl. Math. Sci.*, 6, 6425–6436, <https://doi.org/10.12988/ams.2013.34214>, 2012.
- Ahmed, B.: Landslide susceptibility mapping using multi-criteria evaluation techniques in Chittagong Metropolitan Area, Bangladesh, *Landslides*, 12, 1077–1095, <https://doi.org/10.1007/s10346-014-0521-x>, 2015.
- Ahmed, M. F., Rogers, J. D., and Ismail, E. H.: A regional level preliminary landslide susceptibility study of the upper Indus river basin, *Eur. J. Remote Sens.*, 47, 343–373, <https://doi.org/10.5721/EuJRS20144721>, 2014.
- Akgun, A., Dag, S., and Bulut, F.: Landslide susceptibility mapping for a landslide-prone area (Findikli, NE of Turkey) by likelihood-frequency ratio and weighted linear combination models, *Environ. Geol.*, 54, 1127–1143, <https://doi.org/10.1007/s00254-007-0882-8>, 2008.
- Ali, S., Schneiderwind, S., and Reicherter, K.: Advancing Culture of Living with Landslides, edited by: Mikoš, M., Casagli, N.,

- Yin, Y., and Sassa, K., Springer International Publishing, Cham, Switzerland, 2017.
- Ambraseys, N., Lensen, G., Moinfar, A., and Penningtons, W.: The Pattan (Pakistan) earthquake of 28 December 1974: field observations The earliest known earthquakes of the Northwest Frontier Provinces (NWFP) Geological and tectonic setting Evidence of regional Quaternary and Recent movements, *Q. J. Eng. Geol. Hydrogeol.*, 14, 1–16, 1981.
- Arizapa, J. L., Combalicer, E. A., and Tiburan, C. J. L.: Landslide Susceptibility Mapping of Pagsanjan – Lumban Watershed using GIS and Analytical Hierarchy Process, *Ecosyst. Dev. J.*, 5, 23–32, 2015.
- Ayalew, L., Yamagishi, H., and Ugawa, N.: Landslide susceptibility mapping using GIS-based weighted linear combination, the case in Tsugawa area of Agano River, Niigata Prefecture, Japan, *Landslides*, 1, 73–81, <https://doi.org/10.1007/s10346-003-0006-9>, 2004.
- Ayalew, L., Yamagishi, H., Marui, H. and Kanno, T.: Landslides in Sado Island of Japan: Part II. GIS-based susceptibility mapping with comparisons of results from two methods and verifications, *Eng. Geol.*, 81, 432–445, <https://doi.org/10.1016/j.enggeo.2005.08.004>, 2005.
- Bacha, A. S., Shafique, M., and van der Werff, H.: Landslide inventory and susceptibility modelling using geospatial tools, in Hunza-Nagar valley, northern Pakistan, *J. Mt. Sci.*, 15, 1354–1370, <https://doi.org/10.1007/s11629-017-4697-0>, 2018.
- Bachri, S. and Shresta, R. P.: Landslide hazard assessment using analytic hierarchy processing (AHP) and geographic information system in Kaligesing mountain area of Central Java Province Indonesia, 5th Annu. Int. Work. Expo on Sumatra Tsunami Disaster Recover, 23–24 November 2010, Banda Aceh, Indonesia, 2010.
- Barchi, M., Brozzetti, F., and Lavecchia, G.: Analisi strutturale egeometrica dei bacini della media valle del Tevere e dellavalle umbra, *Boll. Soc. Geol. Ital.*, 110, 65–76, 1993.
- Basharat, M., Shah, H. R., and Hameed, N.: Landslide susceptibility mapping using GIS and weighted overlay method: a case study from NW Himalayas, Pakistan, Arab, *J. Geosci.*, 9, 1–19, <https://doi.org/10.1007/s12517-016-2308-y>, 2016.
- Bishop, M. P., Shroder, J. F., Bonk, R., and Olsenholler, J.: Geomorphic change in high mountains: A western Himalayan perspective, *Global Planet. Change*, 32, 311–329, [https://doi.org/10.1016/S0921-8181\(02\)00073-5](https://doi.org/10.1016/S0921-8181(02)00073-5), 2002.
- Brenning, A.: Spatial prediction models for landslide hazards: review, comparison and evaluation, *Nat. Hazards Earth Syst. Sci.*, 5, 853–862, <https://doi.org/10.5194/nhess-5-853-2005>, 2005.
- Burg, J. P., Jagoutz, O., Dawood, H., and Shahid Hussain, S.: Precollision tilt of crustal blocks in rifted island arcs: Structural evidence from the Kohistan Arc, *Tectonics*, 25, 1–13, <https://doi.org/10.1029/2005TC001835>, 2006.
- Butt, A., Shabbir, R., Ahmad, S. S., and Aziz, N.: Land use change mapping and analysis using Remote Sensing and GIS: A case study of Simly watershed, Islamabad, Pakistan, Egypt. *J. Remote Sens. Sp. Sci.*, 18, 251–259, <https://doi.org/10.1016/j.ejrs.2015.07.003>, 2015.
- Canuti, P., Garduño, V. H., Garzonio, C. A., and Iotti, A.: Slope evolution and mass movements in the Mt. Amiata region (Tuscany, Italy), in: International Workshop on environmental Volcanology, 35–36, Riassunto, 1993.
- Cardinali, M., Galli, M., Guzzetti, F., Reichenbach, P., and Borri, G.: Relazioniframovimenti diversantee fenomenitettonicinel bacino del Torrente Carpina (Umbria settentrionale), *Geogr. Fis. eDinamica Quat.*, 17, 3–17, 1994.
- Cardinali, M., Ardizzone, F., Galli, M., Guzzetti, F., and Reichenbach, P.: Landslides triggered by rapid snow melting: the December 1996–January 1997 event in Central Italy, in: Proceedings Plinius Conference '99, 14–16 October 1999, Maratea, Italy, 439–448, 2000.
- Coco, L. and Buccolini, M.: The Effect of Morphometry, Landuse and Lithology on Landslides Susceptibility: An Exploratory Analysis, IOS Press, 779–784, <https://doi.org/10.3233/978-1-61499-580-7-779>, 2015.
- Deng, X., Li, L., and Tan, Y.: Validation of Spatial Prediction Models for Landslide Susceptibility Mapping by Considering Structural Similarity, *ISPRS Int. J. Geo-Information*, 6, 103, <https://doi.org/10.3390/ijgi6040103>, 2017.
- Derbyshire, E., Fort, M., and Owen, L. A.: Geomorphological hazards along the Karakoram Highway: Khunjerab Pass to the Gilgit River, northernmost Pakistan, *Erdkunde*, 55, 49–71, <https://doi.org/10.3112/erdkunde.2001.01.04>, 2001.
- Ding, L., Qasim, M., Jadoon, I. A. K., Khan, M. A., Xu, Q., Cai, F., Wang, H., Baral, U., and Yue, Y.: The India–Asia collision in north Pakistan: Insight from the U–Pb detrital zircon provenance of Cenozoic foreland basin, *Earth Planet. Sc. Lett.*, 455, 49–61, <https://doi.org/10.1016/j.epsl.2016.09.003>, 2016.
- DiPietro, J. A. and Pogue, K. R.: Tectonostratigraphic subdivisions of the Himalaya: A view from the west, *Tectonics*, 23, TC5001, <https://doi.org/10.1029/2003TC001554>, 2004.
- Dramis, F., Garzonio, C. A., Leoperdi, S., Nanni, T., Pontoni, F., and Rainone, M. L.: Damage due to landslides in the ancient village of Sirolo (Marche, Italy): preliminary analysis of risk mitigation on the historical site., in: Int. Symp. Eng. Geol. of Ancient Work, Monuments and Historical Sites, 19–23 September 1988, Athens, Greece, 1988.
- Ellen, S. D., Mark, R. K., Cannon, S. H., and Knifong, D. L.: Map of Debris-flow Hazard in the Honolulu District of Oahu, Hawaii, U.S. Geological Survey, Washington, D.C., USA, 1993.
- Escape, C. M., Aleman, M. K., Luzon, P. K., and Felix, R.: Comparison of various remote sensing classification methods for landslide detection using ArcGIS, UP NOAH Cent, available at: <https://center.noah.up.edu/ph/comparison-of-various-remote-sensing-classification-methods-for-landslide-detection-using-arcgis/> (last access: 5 March 2017), 2013.
- Fawcett, T.: An introduction to ROC analysis, *Pattern Recognit. Lett.*, 27, 861–874, <https://doi.org/10.1016/j.patrec.2005.10.010>, 2006.
- Fayaz, A., Latif, M., and Khan, K. S. A.: Landslide Evaluation and Stabilization Between Gilgit and Thakot Along the Karakoram Highway, Geological Survey of Pakistan, Islamabad, Pakistan, 1985.
- Fressard, M., Thiery, Y., and Maquaire, O.: Which data for quantitative landslide susceptibility mapping at operational scale? Case study of the Pays d’Auge plateau hillslopes (Normandy, France), *Nat. Hazards Earth Syst. Sci.*, 14, 569–588, <https://doi.org/10.5194/nhess-14-569-2014>, 2014.
- Google Earth Pro: Jijal, Pakistan (October 18, 2014). 35°2'39.38" N, 72°56'22.80" E, Eye alt 3.40 km, 2019

- CNES/Airbus, available at: <https://www.google.com/earth/>, last access: 9 June 2017a.
- Google Earth Pro: Raikot Bridge, Pakistan (October 18, 2014). 35°28'6.88" N, 74°32'57.44" E, Eye alt 5.74 km, 2019 CNES/Airbus, available at: <https://www.google.com/earth/>, last access: 9 June 2017b.
- Google Earth Pro: Attabad, Pakistan (October 18, 2014). 36°17'33.18" N, 74°46'29.82" E, Eye alt 11.69 km, 2019 Digit. Globe, available at: <https://www.google.com/earth/>, last access: 9 June 2017c.
- Goudie, A. S., Brunsdon, D., Collins, D. N., Derbyshire, E., Ferguson, R. I., Hashnet, Z., Jones, D. K. C., Per-Rott, F. A., Said, M., Waters, R. S., and Whalley, W. B.: The geomorphology of the Hunza Valley, Karakoram mountains, Pakistan, *Int. Karakoram-Project*, 2, 359–411, 1984.
- Guzzetti, F., Carrara, A., Cardinali, M., and Reichenbach, P.: Landslide hazard evaluation: A review of current techniques and their application in a multi-scale study, Central Italy, *Geomorphology*, 31, 181–216, [https://doi.org/10.1016/S0169-555X\(99\)00078-1](https://doi.org/10.1016/S0169-555X(99)00078-1), 1999.
- Guzzetti, F., Cardinali, M., Reichenbach, P., and Carrara, A.: Comparing landslide maps: A case study in the upper Tiber River basin, central Italy, *Environ. Manage.*, 25, 247–263, <https://doi.org/10.1007/s002679910020>, 2000.
- Guzzetti, F., Mondini, A. C., Cardinali, M., Fiorucci, F., Santangelo, M., and Chang, K. T.: Landslide inventory maps: New tools for an old problem, *Earth-Sci. Rev.*, 112, 42–66, <https://doi.org/10.1016/j.earscirev.2012.02.001>, 2012.
- Hewitt, K.: Catastrophic landslides and their effects on the Upper Indus streams, Karakoram Himalaya, northern Pakistan, *Geomorphology*, 26, 47–80, [https://doi.org/10.1016/S0169-555X\(98\)00051-8](https://doi.org/10.1016/S0169-555X(98)00051-8), 1998.
- Hu, X. and Cruden, D.: Buckling deformation in the Highwood Pass, Alberta, *Can. Geotech. J.*, 30, 276–286, 1993.
- Intarawichian, N. and Dasananda, S.: Analytical hierarchy process for landslide susceptibility mapping in lower Mae Chaem watershed, Northern Thailand, *Suranaree J. Sci. Technol.*, 17, 277–292, 2010.
- Jade, S.: Estimates of plate velocity and crustal deformation in the Indian subcontinent using GPS geodesy, *Curr. Sci.*, 86, 1443–1448, 2004.
- Kamp, U., Growley, B. J., Khattak, G. A., and Owen, L. A.: GIS-based landslide susceptibility mapping for the 2005 Kashmir earthquake region, *Geomorphology*, 101, 631–642, <https://doi.org/10.1016/j.geomorph.2008.03.003>, 2008.
- Kanwal, S., Atif, S., and Shafiq, M.: GIS based landslide susceptibility mapping of northern areas of Pakistan, a case study of Shigar and Shyok Basins, *Geomat. Nat. Haz. Risk*, 5705, 1–19, <https://doi.org/10.1080/19475705.2016.1220023>, 2016.
- Kartiko, R. D., Brahmantyo, B., and Sadisun, I. A.: Slope and Lithological Controls on Landslide Distribution in West, in: *International Symposium on Geotechnical Hazards: Prevention, Mitigation and Engineering Response*, Utomo, Tohari, Murdohardono, Sadisun, April 2006, Yogyakarta, Indonesia, 177–184, 2006.
- Khan, H., Shafique, M., Khan, M. A., Bacha, M. A., Shah, S. U., and Calligaris, C.: Landslide susceptibility assessment using Frequency Ratio, a case study of northern Pakistan, *Egypt. J. Remote Sens. Sp. Sci.*, 22, 11–24, <https://doi.org/10.1016/j.ejrs.2018.03.004>, 2018.
- Khan, K. S. A., Fayaz, A., Latif, M., and Wazir, A. K.: Rock and Debris Slides Between Khunjrab Pass and Gilgit along the Karakoram Highway, Geological Survey of Pakistan, Islamabad, Pakistan, 1986.
- Khan, K. S. A., Latif, M., Fayaz, A., Khan, N. A., and Khan, S. Z.: Geological Roadlog along the Karakoram Highway from Islamabad to Khunjrab Pass, Geological Survey of Pakistan, Islamabad, Pakistan, 2000.
- Khan, K. S. A., Fayaz, A., Hussain, M., and Latif, M.: Landslides Problems and Their Mitigation along the Karakoram Highway, 1st ed., Geological Survey of Pakistan, Islamabad, Pakistan, 2003.
- Khan, M. A., Jan, M. Q., Windley, B. F., Tarney, J., and Thirlwall, M. F.: The Chilas mafic-ultramafic igneous complex; the root of the Kohistan island arc in the Himalaya of northern Pakistan, *Geol. Soc. Am. Spec. Pap.*, 232, 75–94, 1989.
- Komac, M.: A landslide susceptibility model using the Analytical Hierarchy Process method and multivariate statistics in perialpine Slovenia, *Geomorphology*, 74, 17–28, <https://doi.org/10.1016/j.geomorph.2005.07.005>, 2006.
- Lee, S.: Application of logistic regression model and its validation for landslide susceptibility mapping using GIS and remote sensing data, *Int. J. Remote Sens.*, 26, 1477–1491, <https://doi.org/10.1080/01431160412331331012>, 2005.
- Lee, S., Chwae, U., and Min, K.: Landslide susceptibility mapping by correlation between topography and geological structure: The Janghung area, Korea, *Geomorphology*, 46, 149–162, [https://doi.org/10.1016/S0169-555X\(02\)00057-0](https://doi.org/10.1016/S0169-555X(02)00057-0), 2002.
- Lee, S., Ryu, J.-H., Won, J.-S., and Park, H.-J.: Determination and application of the weights for landslide susceptibility mapping using an artificial neural network, *Eng. Geol.*, 71, 289–302, [https://doi.org/10.1016/S0013-7952\(03\)00142-X](https://doi.org/10.1016/S0013-7952(03)00142-X), 2004.
- Malek, Ž., Zumpano, V., Schröter, D., Glade, T., Balteanu, D., and Micu, M.: Scenarios of land cover change and landslide susceptibility: An example from the buzau subcarpathians, romania, *Eng. Geol. Soc. Territ.*, 5, 743–746, [https://doi.org/10.1007/978-3-319-09048-1\\_144](https://doi.org/10.1007/978-3-319-09048-1_144), 2015.
- MonaLisa, Khwaja, A. A., Jan, M. Q., Yeats, R. S., Hussain, A., and Khan, S. A.: New data on the Indus Kohistan seismic zone and its extension into the Hazara-Kashmir Syntaxis, NW Himalayas of Pakistan, *J. Seismol.*, 13, 339–361, <https://doi.org/10.1007/s10950-008-9117-z>, 2009.
- Nilsen, T. H., Wright, R. H., Vlastic, T. C., and Spangle, W.: Relative slope stability and land-use planning. Selected examples from the San Francisco Bay region, California., *US Geol. Surv. Prof. Pap.*, 944, 1–96, available at: <http://www.scopus.com/inward/record.url?eid=2-s2.0-0018731268&partnerID=tZOTx3y1> (last access: 11 July 2017), 1979.
- Ohlmacher, G. C. and Davis, J. C.: Using multiple logistic regression and GIS technology to predict landslide hazard in northeast Kansas, USA, *Eng. Geol.*, 69, 331–343, [https://doi.org/10.1016/S0013-7952\(03\)00069-3](https://doi.org/10.1016/S0013-7952(03)00069-3), 2003.
- Park, S., Choi, C., Kim, B., and Kim, J.: Landslide susceptibility mapping using frequency ratio, analytic hierarchy process, logistic regression, and artificial neural network methods at the Inje area, Korea, *Environ. Earth Sci.*, 68, 1443–1464, <https://doi.org/10.1007/s12665-012-1842-5>, 2013.
- Pourghasemi, H. R. and Rossi, M.: Landslide susceptibility modeling in a landslide prone area in Mazandarn Province,

- north of Iran: a comparison between GLM, GAM, MARS, and M-AHP methods, *Theor. Appl. Climatol.*, 130, 609–633, <https://doi.org/10.1007/s00704-016-1919-2>, 2017.
- Pourghasemi, H. R., Pradhan, B., and Gokceoglu, C.: Application of fuzzy logic and analytical hierarchy process (AHP) to landslide susceptibility mapping at Haraz watershed, Iran, *Nat. Hazards*, 63, 965–996, <https://doi.org/10.1007/s11069-012-0217-2>, 2012.
- Pourghasemi, H. R., Beheshtirad, M., and Pradhan, B.: A comparative assessment of prediction capabilities of modified analytical hierarchy process (M-AHP) and Mamdani fuzzy logic models using Netcad-GIS for forest fire susceptibility mapping, *Geomat. Nat. Haz. Risk*, 7, 861–885, <https://doi.org/10.1080/19475705.2014.984247>, 2016.
- Pradhan, B., Lee, S., and Buchroithner, M. F.: Remote Sensing and GIS-based Landslide Susceptibility Analysis and its Cross-validation in Three Test Areas Using a Frequency Ratio Model, *Photogramm. Fernerkun.*, 2010, 17–32, <https://doi.org/10.1127/1432-8364/2010/0037>, 2010.
- Rahim, I., Ali, S. M., and Aslam, M.: GIS Based Landslide Susceptibility Mapping with Application of Analytical Hierarchy Process in District Ghizer, Gilgit Baltistan Pakistan, *J. Geosci. Environ. Prot.*, 06, 34–49, <https://doi.org/10.4236/gep.2018.62003>, 2018.
- Reichenbach, P., Busca, C., Mondini, A. C., and Rossi, M.: The Influence of Land Use Change on Landslide Susceptibility Zonation: The Briga Catchment Test Site (Messina, Italy), *Environ. Manage.*, 54, 1372–1384, <https://doi.org/10.1007/s00267-014-0357-0>, 2014.
- Reis, S.: Analyzing land use/land cover changes using remote sensing and GIS in Rize, North-East Turkey, *Sensors*, 8, 6188–6202, <https://doi.org/10.3390/s8106188>, 2008.
- Restrepo, C. and Alvarez, N.: Landslides and their contribution to land-cover change in the mountains of Mexico and Central America, *Biotropica*, 38, 446–457, <https://doi.org/10.1111/j.1744-7429.2006.00178.x>, 2006.
- Roslee, R., Mickey, A. C., Simon, N., and Norhisham, M. N.: Landslide Susceptibility Analysis (Lsa) Using Weighted Overlay Method (Wom) Along the Genting Sempah To Bentong Highway, Pahang, Malays. *J. Geosci.*, 1, 13–19, <https://doi.org/10.26480/mjg.02.2017.13.19>, 2017.
- Rozos, D., Bathrellos, G. D., and Skillodimou, H. D.: Comparison of the implementation of rock engineering system and analytic hierarchy process methods, upon landslide susceptibility mapping, using GIS: A case study from the Eastern Achaia County of Peloponnesus, GREECE, *Environ. Earth Sci.*, 63, 49–63, <https://doi.org/10.1007/s12665-010-0687-z>, 2011.
- Ruff, M. and Czurda, K.: Landslide susceptibility analysis with a heuristic approach in the Eastern Alps (Vorarlberg, Austria), *Geomorphology*, 94, 314–324, <https://doi.org/10.1016/j.geomorph.2006.10.032>, 2008.
- Rwanga, S. S. and Ndambuki, J. M.: Accuracy Assessment of Land Use/Land Cover Classification Using Remote Sensing and GIS, *Int. J. Geosci.*, 08, 611–622, <https://doi.org/10.4236/ijg.2017.84033>, 2017.
- Saaty, R. W.: The analytic hierarchy process-what it is and how it is used, *Math. Model.*, 9, 161–176, [https://doi.org/10.1016/0270-0255\(87\)90473-8](https://doi.org/10.1016/0270-0255(87)90473-8), 1987.
- Saaty, T. L.: How to make a decision: The analytic hierarchy process, *Eur. J. Oper. Res.*, 48, 9–26, [https://doi.org/10.1016/0377-2217\(90\)90057-I](https://doi.org/10.1016/0377-2217(90)90057-I), 1990.
- Sarkar, S. and Kanungo, D. P.: An integrated approach for landslide susceptibility mapping using remote sensing and GIS, *Photogramm. Eng. Remote Sens.*, 70, 617–628, <https://doi.org/10.14358/PERS.70.5.617>, 2004.
- Searle, M. P., Khan, M. A., Fraser, J. E., Gough, S. J., and Jan, M. Q.: The tectonic evolution of the Kohistan-Karakoram collision belt along the Karakoram Highway transect, north Pakistan, *Tectonics*, 18, 929–949, 1999.
- Shahabi, H. and Hashim, M.: Landslide susceptibility mapping using GIS-based statistical models and Remote sensing data in tropical environment, *Sci. Rep.*, 5, 9899, <https://doi.org/10.1038/srep09899>, 2015.
- Shit, P. K., Bhunia, G. S., and Maiti, R.: Potential landslide susceptibility mapping using weighted overlay model (WOM), *Model. Earth Syst. Environ.*, 21, 1–10, <https://doi.org/10.1007/s40808-016-0078-x>, 2016.
- Soeters, R. and van Westen, C. J.: Slope instability recognition, analysis, and zonation, in: *Landslides, investigation and mitigation*, edited by: Turner, A. K. and Schuster, R. L., Washington, D.C., USA, 1996.
- Süzen, M. L. and Doyuran, V.: A comparison of the GIS based landslide susceptibility assessment methods: Multivariate versus bivariate, *Environ. Geol.*, 45, 665–679, <https://doi.org/10.1007/s00254-003-0917-8>, 2004.
- Taherynia, M. H., Mohammadi, M., and Ajalloeian, R.: Assessment of Slope Instability and Risk Analysis of Road Cut Slopes in Lashotor Pass, Iran, *J. Geol. Res.*, 2014, 1–12, <https://doi.org/10.1155/2014/763598>, 2014.
- Tahirkheli, R. A. K. and Jan, M. Q.: Geology of Kohistan, Karakoram Himalaya, northern Pakistan, *Geol. Bull. Univ. Peshawar, Pakistan*, 11, 1–30, 1979.
- Treloar, P. J., Petterson, M. G., Jan, M. Q., and Sullivan, M. A.: A re-evaluation of the stratigraphy and evolution of the Kohistan arc sequence, Pakistan Himalaya: implications for magmatic and tectonic arc-building processes, *J. Geol. Soc.*, 153, 681–693, <https://doi.org/10.1144/gsjgs.153.5.0681>, 1996.
- Ulbricht, K. A., Teotia, H. S., and Civco, D. L.: Supervised Classification to Land Cover Mapping in Semi-Arid Environment of NE Brazil Using Landsat-TM and SPOT Data, *Int. Arch. Photogramm. Remote Sens.*, 29, 821–821, available at: [http://www.isprs.org/proceedings/XXIX/congress/part7/821\\_XXIX-part7.pdf](http://www.isprs.org/proceedings/XXIX/congress/part7/821_XXIX-part7.pdf) (last access: 16 February 2016), 1993.
- USGS Earthquake Catalog: USGS Earthquake Catalog, *Earthq. Cat.*, available at: <https://earthquake.usgs.gov/earthquakes/search/>, last access: 23 July 2017.
- Vakhshoori, V. and Zare, M.: Is the ROC curve a reliable tool to compare the validity of landslide susceptibility maps?, *Geomat. Nat. Haz. Risk*, 9, 249–266, <https://doi.org/10.1080/19475705.2018.1424043>, 2018.
- Vallejo, G. L. and Ferrer, M.: *Geological Engineering*, 1st ed., CRC Press/Balkema, AK Leiden, the Netherlands, 2011.
- van Westen, C. J., van Asch, T. W. J., and Soeters, R.: Landslide hazard and risk zonation - Why is it still so difficult?, *Bull. Eng. Geol. Environ.*, 65, 167–184, <https://doi.org/10.1007/s10064-005-0023-0>, 2006.

- Varnes, D. J.: Slope movements types and processes, in: Landslides analysis and control, edited by: Schuster, R. L. and Krizek, R. J., Washington, D.C., USA, 1978.
- Wang, Q., Li, W., Chen, W., and Bai, H.: GIS-based assessment of landslide susceptibility using certainty factor and index of entropy models for the Qianyang county of Baoji city, China, *J. Earth Syst. Sci.*, 124, 1399–1415, 2015.
- Williams, M. P.: The Geology of the Besham area, North Pakistan: Deformation and Imbrication in the footwall of the Main Mantle Thrust, *Geol. Bull. Univ. Peshawar*, 22, 65–82, 1989.
- Yalcin, A.: GIS-based landslide susceptibility mapping using analytical hierarchy process and bivariate statistics in Ardesen (Turkey): Comparisons of results and confirmations, *Catena*, 72, 1–12, <https://doi.org/10.1016/j.catena.2007.01.003>, 2008.
- Zeitler, P. K.: Cooling history of the NW Himalaya, Pakistan, *Tectonics*, 4, 127–151, <https://doi.org/10.1029/TC004i001p00127>, 1985.
- Zhiquan, Y. and Yingyan, Z.: Types and Space Distribution Characteristics of Debris Flow Disasters Along China-Pakistan Highway, *Electron. J. Geotech. Eng.*, 21, 191–200, 2016.
- Zhou, S., Chen, G., Fang, L., and Nie, Y.: GIS-based integration of subjective and objective weighting methods for regional landslides susceptibility mapping, *Sustain.*, 8, 1–15, <https://doi.org/10.3390/su8040334>, 2016.